small percentage of mdx myofibers improved the mdx phenotype. *Mol Ther* **10**: 821–828.
26. Fabb, SA, Wells, DJ, Serpente, P and Dickson, G (2002). Adeno-associated virus vector gene transfer and sarcolemmal expression of a 144 kDa micro-dystrophin effectively restores the dystrophin-associated protein complex and inhibits myofibre degeneration in nude/mdx mice. *Hum Mol Genet* **11**: 733–741.
27. Harper, SQ, Hauser, MA, DelloRusso, C, Duan, D, Crawford, RW, Phelps, SF *et al.* (2002). Modular flexibility of dystrophin: implications for gene therapy of Duchenne muscular dystrophy. *Nat Med* **8**: 253–261.
28. Acsadi, G, Dickson, G, Love, DR, Jani, A, Walsh, FS, Gurusinghe, A *et al.* (1991). Human dystrophin expression in mdx mice after intramuscular injection of DNA constructs. *Nature* **352**: 815–818.
29. Quenneville, SP, Chapdelaine, P, Rousseau, J, Beaulieu, J, Caron, NJ, Skuk, D *et al.* (2004). Nucleofection of muscle-derived stem cells and myoblasts with phiC31 integrase: stable expression of a full-length-dystrophin fusion gene by human myoblasts. *Mol Ther* **10**: 679–687.
30. Li, S, Kimura, E, Fall, BM, Reyes, M, Angello, JC, Welikson, R *et al.* (2005). Stable transduction of myogenic cells with lentiviral vectors expressing a minidystrophin. *Gene Ther* **12**: 1099–1108.
31. Quenneville, SP, Chapdelaine, P, Skuk, D, Paradis, M, Goulet, M, Rousseau, J *et al.* (2007). Autologous transplantation of muscle precursor cells modified with a lentivirus for muscular dystrophy: human cells and primate models. *Mol Ther* **15**: 431–438.
32. Bachrach, E, Li, S, Perez, AL, Schienda, J, Liadaki, K, Volinski, J *et al.* (2004). Systemic delivery of human microdystrophin to regenerating mouse dystrophic muscle by muscle progenitor cells. *Proc Natl Acad Sci USA* **101**: 3581–3586.
33. Sampaolesi, M, Torrente, Y, Innocenzi, A, Tonlorenzi, R, D'Antona, G, Pellegrino, MA *et al.* (2003). Cell therapy of alpha-sarcoglycan null dystrophic mice through intra-arterial delivery of mesoangioblasts. *Science* **301**: 487–492.
34. Sampaolesi, M, Blot, S, D'Antona, G, Granger, N, Tonlorenzi, R, Innocenzi, A *et al.* (2006). Mesoangioblast stem cells ameliorate muscle function in dystrophic dogs. *Nature* **444**: 574–579.
35. Fukada, S, Higuchi, S, Segawa, M, Koda, K, Yamamoto, Y, Tsujikawa, K *et al.* (2004). Purification and cell-surface marker characterization of quiescent satellite cells from murine skeletal muscle by a novel monoclonal antibody. *Exp Cell Res* **296**: 245–255.
36. Zammit, PS, Golding, JP, Nagata, Y, Hudon, V, Partridge, TA and Beauchamp, JR (2004). Muscle satellite cells adopt divergent fates: a mechanism for self-renewal? *J Cell Biol* **166**: 347–357.
37. Yablonka-Reuveni, Z and Rivera, AJ (1994). Temporal expression of regulatory and structural muscle proteins during myogenesis of satellite cells on isolated adult rat fibers. *Dev Biol* **164**: 588–603.
38. Cornelison, DD and Wold, BJ (1997). Single-cell analysis of regulatory gene expression in quiescent and activated mouse skeletal muscle satellite cells. *Dev Biol* **191**: 270–283.
39. Rando, TA and Blau, HM (1994). Primary mouse myoblast purification, characterization, and transplantation for cell-mediated gene therapy. *J Cell Biol* **125**: 1275–1287.
40. Burns, JC, Friedmann, T, Driever, W, Burrascano, M and Yee, JK (1993). Vesicular stomatitis virus G glycoprotein pseudotyped retroviral vectors: concentration to very high titer and efficient gene transfer into mammalian and nonmammalian cells. *Proc Natl Acad Sci USA* **90**: 8033–8037.
41. Nagai, T, Ibata, K, Park, ES, Kubota, M, Mikoshiba, K and Miyawaki, A (2002). A variant of yellow fluorescent protein with fast and efficient maturation for cell-biological applications. *Nat Biotechnol* **20**: 87–90.
42. Smythe, GM, Hodgetts, SI and Grounds, MD (2001). Problems and solutions in myoblast transfer therapy. *J Cell Mol Med* **5**: 33–47.
43. Hashimoto, N, Murase, T, Kondo, S, Okuda, A and Inagawa-Ogashiwa, M (2004). Muscle reconstitution by muscle satellite cell descendants with stem cell-like properties. *Development* **131**: 5481–5490.
44. Kobinger, GP, Louboutin, JP, Barton, ER, Sweeney, HL and Wilson, JM (2003). Correction of the dystrophic phenotype by *in vivo* targeting of muscle progenitor cells. *Hum Gene Ther* **14**: 1441–1449.
45. Mouly, V, Aamiri, A, Perie, S, Mamchaoui, K, Barani, A, Bigot, A *et al.* (2005). Myoblast transfer therapy: is there any light at the end of the tunnel? *Acta Myol* **24**: 128–133.
46. Kameya, S, Miyagoe, Y, Nonaka, I, Ikemoto, T, Endo, M, Hanaoka, K *et al.* (1999). Alpha1-syntrophin gene disruption results in the absence of neuronal-type nitric-oxide synthase at the sarcolemma but does not induce muscle degeneration. *J Biol Chem* **274**: 2193–2200.
47. Miyoshi, H, Blomer, U, Takahashi, M, Gage, FH and Verma, IM (1998). Development of a self-inactivating lentivirus vector. *J Virol* **72**: 8150–8157.
48. Naldini, L, Blomer, U, Gallay, P, Ory, D, Mulligan, R, Gage, FH *et al.* (1996). *In vivo* gene delivery and stable transduction of nondividing cells by a lentiviral vector. *Science* **272**: 263–267.
49. Dull, T, Zufferey, R, Kelly, M, Mandel, RJ, Nguyen, M, Trono, D *et al.* (1998). A third-generation lentivirus vector with a conditional packaging system. *J Virol* **72**: 8463–8471.

STEM CELLS®
TISSUE-SPECIFIC STEM CELLS

Molecular Signature of Quiescent Satellite Cells in Adult Skeletal Muscle

SO-ICHIRO FUKADA,[a] AKIYOSHI UEZUMI,[a] MADOKA IKEMOTO,[a] SATORU MASUDA,[a] MASASHI SEGAWA,[b] NAOKI TANIMURA,[c] HIROSHI YAMAMOTO,[b] YUKO MIYAGOE-SUZUKI,[a] SHIN'ICHI TAKEDA[a]

[a]Department of Molecular Therapy, National Institute of Neuroscience, National Center of Neurology and Psychiatry, Tokyo, Japan; [b]Department of Immunology, Graduate School of Pharmaceutical Sciences, Osaka University, Osaka, Japan; [c]Bio and Nano Technologies, Science and Technology Division, Mizuho Information & Research Institute Inc., Tokyo, Japan

Key Words. Fluorescence-activated cell sorting • Microarray • Quiescence • Muscle satellite cells • Calcitonin receptor

ABSTRACT

Skeletal muscle satellite cells play key roles in postnatal muscle growth and regeneration. To study molecular regulation of satellite cells, we directly prepared satellite cells from 8- to 12-week-old C57BL/6 mice and performed genome-wide gene expression analysis. Compared with activated/cycling satellite cells, 507 genes were highly upregulated in quiescent satellite cells. These included negative regulators of cell cycle and myogenic inhibitors. Gene set enrichment analysis revealed that quiescent satellite cells preferentially express the genes involved in cell-cell adhesion, regulation of cell growth, formation of extracellular matrix, copper and iron homeostasis, and lipid transportation. Furthermore, reverse transcription-polymerase chain reaction on differentially expressed genes confirmed that calcitonin receptor (CTR) was exclusively expressed in dormant satellite cells but not in activated satellite cells. In addition, CTR mRNA is hardly detected in nonmyogenic cells. Therefore, we next examined the expression of CTR in vivo. CTR was specifically expressed on quiescent satellite cells, but the expression was not found on activated/proliferating satellite cells during muscle regeneration. CTR-positive cells reappeared at the rim of regenerating myofibers in later stages of muscle regeneration. Calcitonin stimulation delayed the activation of quiescent satellite cells. Our data provide roles of CTR in quiescent satellite cells and a solid scaffold to further dissect molecular regulation of satellite cells. STEM CELLS *2007;25:2448–2459*

Disclosure of potential conflicts of interest is found at the end of this article.

INTRODUCTION

Muscle satellite cells, which account for 2%–5% of the total nuclei in adult skeletal muscle, play a major role in muscle regeneration [1, 2]. Under normal conditions, satellite cells are found external to the myofiber plasma membrane and beneath the muscle basal lamina [3] and are mitotically quiescent in the adult skeletal muscle [4, 5]. When activated by muscle damage, they proliferate, differentiate, fuse with each other or injured fibers, and eventually regenerate mature myofibers under the influence of innervation [6]. Recently, it was clearly demonstrated that the proliferation capacity of satellite cells in vivo is robust and that the contribution of interstitial cells or bone marrow-derived cells to muscle fiber regeneration is limited [7]. Importantly, a small fraction of activated satellite cells exit the cell cycle and return to the quiescent satellite state during muscle regeneration to maintain their numbers and the regenerative capacity of muscle.

Besides muscle fiber repair, satellite cells are also responsible for postnatal growth [8] and hypertrophy of skeletal muscle [9], and impairment of their functions is related to several pathological conditions, for example, muscular dystrophies and aging-related muscle atrophy [10]. Moreover, several studies showed that satellite cells differentiate into adipogenic cells or osteocytes in vitro [11–13], implying that they contribute to the fatty infiltration seen in Duchenne muscular dystrophy. Thus, normal functioning of satellite cells is indispensable for the integrity of skeletal muscle, and the cells themselves are an important source of cells for cell therapy of muscle diseases, making it valuable to clarify the molecular regulation of maintenance, activation/proliferation, and differentiation in satellite cells.

Like hematopoietic stem cells, most satellite cells are in a quiescent and undifferentiated state in the adult. Although quiescence is important to retain the proliferative and differentiative potential of satellite cells throughout the lifetime, the molecular regulation of quiescence remains poorly defined. Recent studies suggested that myostatin, a skeletal muscle-specific transforming growth factor-β superfamily member, suppresses the activation of satellite cells [14]. Myostatin has been shown to induce a potent cyclin-dependent kinase inhibitor, p21(Cdkn1a), in vitro [15]. Other in vitro studies suggested that the decrease of MyoD protein and induction of another cyclin-dependent kinase inhibitor, p27(Cdkn1b) [16], and a Rb-related pocket protein, p130 [16, 17], are involved in the attainment of quiescence by proliferating myoblasts.

Correspondence: Yuko Miyagoe-Suzuki, M.D., Ph.D., Department of Molecular Therapy, National Institute of Neuroscience, National Center of Neurology and Psychiatry, 4-1-1 Ogawa-higashi, Kodaira, Tokyo 187-8502, Japan. Telephone: +81-42-346-1720; Fax: +81-42-346-1750; e-mail: miyagoe@ncnp.go.jp Received January 8, 2007; accepted for publication June 19, 2007; first published online in STEM CELLS *EXPRESS* June 28, 2007. 1066-5099/2007/$30.00/0 doi: 10.1634/stemcells.2007-0019

We previously reported a method to purify quiescent satellite cells from adult skeletal muscle using the fluorescence-activated cell sorting (FACS) technique and a novel antibody named SM/C-2.6 [18]. In this study, to clarify the molecular regulation of quiescent satellite cells, we performed genome-wide gene expression profiling of quiescent satellite cells isolated from C57BL/6 mice. Expression analysis of individual genes identified several candidate genes that regulate dormancy of satellite cells. Gene set enrichment analysis (GSEA) revealed that the gene sets involved in cell-cell adhesion, cell growth, copper and iron ion homeostasis, lipid transport, and formation of extracellular matrix were coordinately upregulated in quiescent satellite cells. Furthermore, we demonstrate that calcitonin receptor (CTR) is expressed specifically on quiescent satellite cells in vivo and that calcitonin significantly attenuates the activation of satellite cells. Our study is the first report of in-depth gene expression analysis of quiescent satellite cells and will greatly facilitate the investigation of molecular regulation of satellite cells in both physiological and pathological conditions.

MATERIALS AND METHODS

Animals

All procedures using experimental animals were approved by the Experimental Animal Care and Use Committee at the National Institute of Neuroscience. C57BL/6 mice were purchased from Nihon CLEA (Tokyo, http://www.clea-japan.com).

Preparation of Satellite Cells and Nonmyogenic Cells from Mouse Limb Muscles

Mononuclear cells were prepared from fore- and hindlimb muscles of 8- to 12-week-old female C57BL/6 mice as described [19] and incubated on ice for 30 minutes in the presence of a 1:200 dilution of phycoerythrin-conjugated anti-CD45 (clone: 30-F11) and biotinylated SM/C-2.6 [18]. Cells were then incubated with streptavidin-labeled allophycocyanin on ice for 30 minutes and resuspended in phosphate-buffered saline (PBS) containing 2% fetal bovine serum (FBS) and 2 μg/ml propidium iodide (PI). Cell sorting was performed on a FACSVantage SE flow cytometer (BD Biosciences, San Diego, http://www.bdbiosciences.com). Dead cells were excluded by PI gating. All antibodies and reagents for FACS analysis were purchased from BD Pharmingen (San Diego, http://www.bdbiosciences.com/index_us.shtml).

Cell Culture

Satellite cells were cultured in growth medium consisting of high-glucose Dulbecco's modified Eagle's medium (DMEM; Invitrogen, Carlsbad, CA, http://www.invitrogen.com) containing 20% fetal calf serum (FCS; Trace Biosciences, New South Wales, Australia), 2.5 ng/ml basic fibroblast growth factor (Invitrogen), and penicillin (100 U/ml)-streptomycin (100 μg/ml) (Gibco-BRL, Gaithersburg, MD, http://www.gibcobrl.com) on culture dishes coated with Matrigel (BD Biosciences). Single living myofibers were prepared as described [20] and transferred to Matrigel-coated 24-well culture dishes (one fiber per well). After a 2-day culture in growth medium with or without elcatonin, satellite cells that had detached from muscle fibers were counted.

Immunocytochemical Analysis

FACS-sorted cells were collected on glass slides by Cytospin 3 (Thermo Shandon Inc., Pittsburgh, http://www.thermo.com) and immunostained as described [19]. Cultured cells were fixed on 8-well Lab-Tek Chamber Slides (Nunc, Rochester, NY, http://www.nuncbrand.com) and stained as described [19, 21] with mouse anti-Pax7 (1:100; clone: Pax7; Developmental Studies Hybridoma Bank, Iowa City, IA, http://www.uiowa.edu/~dshbwww), mouse anti-MyoD (1:200; clone: 5.8A; NeoMarkers; Lab Vision, Fremont, CA, http://www.labvision.com), mouse anti-myogenin (1:100; clone: F5D; Developmental Studies Hybridoma Bank), rabbit anti-Ki67 (1:2; Ylem, Rome), or rabbit anti-p57 antibodies (1:50; GeneTex, San Antonio, http://www.genetex.com) at 4°C overnight and then reacted with secondary antibodies conjugated with Alexa 488 or Alexa 568 (Molecular Probes, Eugene, OR, http://probes.invitrogen.com). Nuclei were stained with 4,6-diamidino-2-phenylindole (DAPI). Images were photographed using a phase-contrast and fluorescence microscope IX70 (Olympus, Tokyo, http://www.olympus-global.com) equipped with a Quantix air-cooled CCD camera (Photometrics, Kew, VIC, Australia, http://www.photometrix.com.au) and IP Lab software (Scanalytics, Rockville, MD, http://www.scanalytics.com).

Immunohistochemistry

Immunostaining of muscle cryosections was performed as previously described [21] using rat anti-laminin α2 (1:200; clone 4H8-2; Alexis Biochemical, Lausen, Switzerland, http://www.axxora.com), rabbit anti-M-cadherin [21], rabbit anti-human CTR (1:200; Serotec Ltd., Oxford, U.K., http://www.serotec.com), goat anti-Notch 3 (1:100; R&D Systems Inc., Minneapolis, http://www.rndsystems.com), or mouse anti-Pax7. Rabbit anti-mouse HeyL polyclonal antibody was produced in our laboratory. In brief, the DNA fragment corresponding to amino acids 220–287 of mouse HeyL (GenBank: NM_013905) was fused to glutathione *S*-transferase in the pGEX-1 Lambda T vector (GE Healthcare, Uppsala, Sweden, http://www.gehealthcare.com). The purified fusion protein was used to immunize New Zealand White rabbits. The obtained serum was affinity-purified. For Pax7 staining, an M.O.M. kit (Vector Laboratories, Burlingame, CA, http://www.vectorlabs.com) was used to block endogenous mouse IgG. For CTR staining, horseradish peroxidase-conjugated anti-rabbit IgG donkey secondary antibody (1:100; GE Healthcare) and Alexa 568-conjugated Tyramid (Molecular Probes) were used to amplify the signal. Nuclei were counterstained with TOTO-3 (1:5,000; Molecular Probes) or DAPI. The images were recorded using a confocal laser scanning microscope system TCSSP (Leica, Heerbrugg, Switzerland, http://www.leica.com) or Axiophot microscope (Carl Zeiss, Jena, Germany, http://www.zeiss.com).

Cell Cycle Analysis

Muscle-derived mononucleated cells or cultured SM/C-2.6 positive cells were suspended at 10^6 cells per milliliter in DMEM (Invitrogen) containing 2% FBS (Trace Biosciences), 10 mM Hepes, and 10 μM Hoechst 33342 (Sigma-Aldrich, St. Louis, http://www.sigmaaldrich.com) and incubated for 45 minutes at 37°C. An additional incubation was performed in the presence of 10 μg/ml Pyronin Y (Sigma-Aldrich) for 45 minutes at 37°C. Cells were then washed with PBS containing 2% FCS. Muscle-derived mononucleated cells were stained with SM/C-2.6 antibody and analyzed by FACSVantage SE flow cytometer.

Cell Proliferation Assay

After cell sorting, quiescent satellite cells were plated on 96-well culture plates at a density of 3,000–8,000 in the absence or presence of elcatonin (0.01–0.1 U/ml) (Asahi Kasei Pharma Corporation, Tokyo, http://www.asahi-kasei.co.jp/asahi/en) and cultured for 1–2 days. Then 5-bromo-2′-deoxyuridine (BrdU) (10 μM) was added to the culture. To examine the effects of elcatonin on activated satellite cells, satellite cells were cultured for 3 days and then elcatonin was added to the culture 24 hours before addition of BrdU. Twenty-four hours later, BrdU uptake was quantified by cell proliferation enzyme-linked immunosorbent assay, BrdU Kit (Roche Diagnostics, Basel, Switzerland, http://www.roche-applied-science.com), and lumi-Image F1 (Roche). In Figure 6B, cells were exposed to elcatonin for 30 minutes and washed twice with PBS and then plated on culture dishes.

Detection of Apoptotic Cells

Cells were cultured on 8-well Lab-Tek chamber slides with or without elcatonin. Apoptotic cells were detected by rhodamine fluorescence using an ApopTag Red In Situ Apoptosis Detection Kit (Chemicon, Temecula, CA, http://www.chemicon.com).

RNA Extraction and Reverse Transcription-Polymerase Chain Reaction

Total RNA was extracted from sorted or cultured cells with a Qiagen RNeasy Mini kit according to the manufacturer's instructions (Qiagen, Hilden, Germany, http://www1.qiagen.com) and then reverse-transcribed into cDNA by using TaqMan Reverse Transcription Reagents (Roche). The polymerase chain reaction (PCR) was performed with cDNA products under the following cycling conditions: 94°C for 3 minutes followed by 30–40 cycles of amplification, annealing, and extension (94°C for 15 seconds, 58°C for 30 seconds, and 72°C for 30 seconds) with a final incubation at 72°C for 5 minutes. Specific primer sequences used for PCR are described in supplemental online Materials and Methods.

Target Synthesis, Gene Chip Hybridization, and Data Acquisition

To label antisense RNA (aRNA) with biotin for microarray hybridization, we followed the protocol supplied by the manufacturer (Affymetrix, Santa Clara, CA, http://www.affymetrix.com). Because the starting amount of total RNA was 100 ng for the sorted SM/C-2.6$^+$ cell fraction, we used a two-cycle biotin aRNA synthesis kit (Affymetrix). Labeled aRNA was fragmented according to Affymetrix GeneChip protocol and then hybridized to Affymetrix MOE430A GeneChip arrays for 16 hours. After washing, the gene chips were stained according to the instrument's standard Eukaryotic GE WS2v4 protocol using antibody-mediated signal amplification. The signal was determined, using the Microarray Suite (MAS) 5.0 absolute analysis algorithm, as the average fluorescence intensity among the intensities obtained from the probe set. The signal of a probe set was calculated as the one-step biweight estimate of combined differences of all the probe pairs (perfectly matched and mismatched) in the probe set. A one-sided Wilcoxon's signed rank test was used to calculate a p value that reflects the significance of differences between perfectly matched and mismatched probe pairs. The p value was used to make the absolute call for probe sets. A "Present" call was assigned to transcripts for p values between 0 and .04, a "Marginal" call was assigned to transcripts for p values between .04 and .06, and an "Absent" call was assigned to transcripts for p values between .06 and 1.0.

Microarray Data Analysis

Scanned output files were analyzed by the probe level analysis package MAS 5.0 (Affymetrix). The Present/Absent call provided by the Affymetrix programs was used for the first selection. The MAS 5.0-generated raw data were uploaded to GeneSpring software version 7.0 (Silicongenetics, Redwood, CA, http://www.chem.agilent.com/scripts/PHome.asp). Data normalization was achieved by one of two methods: (a) each signal was divided by the 50th percentile of all signals in a specific hybridization experiment or (b) each signal was divided by the median of its values in all samples. A more reliable list of "5-fold changing" genes was obtained by applying the filtering options of GeneSpring. Present calls in all (four) quiescent or activated satellite cell probes were selected and a restriction, which passed genes with raw data above 100, was applied. Then, using all the quiescent and activated satellite cells as data, we performed a one-way analysis of variance test between the quiescent satellite cell group and the activated satellite cell group. In particular, a parametric test, with variances assumed equal (Student's t test, p value cut-off .05; multiple testing correction: Benjamini and Hochberg false discovery rate), was applied. The genes passing all these filters and tests were selected as "5-fold changing genes." Nonmyogenic cells (SM/C-2.6$^-$/CD45$^-$ cells) were also prepared four times.

Gene Set Enrichment Analysis

GSEA [22] is a statistical analysis of sets of gene expression profiles, separated by phenotypic labels. Using GSEA, we can test hypotheses concerned with predefined sets of genes; the rank orderings of the genes in the whole gene set calculated with a given ranking method are random with regard to a given classification of samples. As a result of the analysis, nominal p values, family-wise error rate p values, and false discovery rate (FDR) q values for test hypotheses (thus for gene sets) were obtained.

In our analysis, we used the GSEA-P software package [22], which is available from the Broad Institute (Cambridge, MA, http://www.broad.mit.edu). We prepared, as input to the GSEA-P, the MAS 5.0-generated raw signal data and gene sets derived independently. We chose genes on the chip that were detected (the Present call was assigned) in at least one sample (17,150 of 22,626). The raw signals of the chosen genes were normalized so that their total sum was 1. Because the total amount of mRNA in a quiescent satellite cell (QSC) is much less than that in an activated satellite cell (ASC), the normalized signal should be understood as a relative signal among the chosen genes. To compile the gene sets, we assigned each probe to a gene ontology (GO) category [23] using annotations of the MOE430A chip (September 22, 2005) provided by Affymetrix. Therefore, these gene sets reflect the structure of the GO categories and subcategories of molecular function (MF), biological process (BP), and cellular component (CC). The 17,150 genes chosen comprised 1,674, 1,698, and 412 gene sets in the MF, BP, and CC subcategories, respectively, and were reduced to 162, 218, and 85 after filtering out gene sets with sizes smaller than 20 or larger than 1,000. We ran the GSEA-P with the signal-to-noise option for its ranking metric, with permutation over phenotype labels of QSC and ASC samples, and repeated it 2,000 times with the "weighted" option for its scoring scheme.

Results and Discussion

Isolation of Quiescent Satellite Cells from Mouse Skeletal Muscle

First, to obtain RNA samples for microarray analysis, we prepared mononuclear cells from 8- to 12-week-old C57BL/6 mouse muscle, and the SM/C-2.6$^+$ fraction was collected as the satellite cell fraction by FACS [18] (Fig. 1A). Consistent with our previous report, more than 97% of fresh SM/C-2.6$^+$ cells expressed Pax7 (Fig. 1B) but were mostly negative for both MyoD (Fig. 1Ca, 1Cb) and Ki67 (Fig. 1Ce, 1Cf). After 4–5 days of culture, more than 98% of SM/C-2.6$^+$ cells expressed MyoD (Fig. 1Cg, 1Ch) and Ki67 (Fig. 1Ck, 1Cl). Both freshly isolated, uncultured SM/C-2.6$^+$ cells and SM/C-2.6$^+$ cells cultured in growth medium were negative for myogenin expression (Fig. 1Cc, 1Cd, 1Ci, 1Cj), but these cells started to express myogenin and differentiated well into multinucleated myotubes after mitogen withdrawal (data not shown). In contrast, more than 99% of freshly isolated SM/C-2.6$^-$/CD45$^-$ cells were negative for Pax7 expression (Fig. 1Bc, 1Bd), and cultured SM/C-2.6$^-$/CD45$^-$ cells did not express MyoD (data not shown), again indicating that myogenic cells are highly enriched in the SM/C-2.6$^+$ fraction.

The forward and side scatter profiles of freshly isolated SM/C-2.6$^+$ cells showed that they are small and uniform in granularity (data not shown). In fact, as shown in Figure 1D, the cell size of fresh SM/C-2.6$^+$ cells was estimated to be approximately one-half that of cultured SM/C-2.6$^+$ cells based on the forward scatter profile, indicating that the freshly isolated SM/C-2.6$^+$ cells were not activated yet. Pyronin Y staining showed the small amount of RNA content in freshly isolated SM/C-2.6$^+$ cells (Fig. 1D). In general, a Pyronin^{low} and Hoechst 33342^{low} fraction is considered

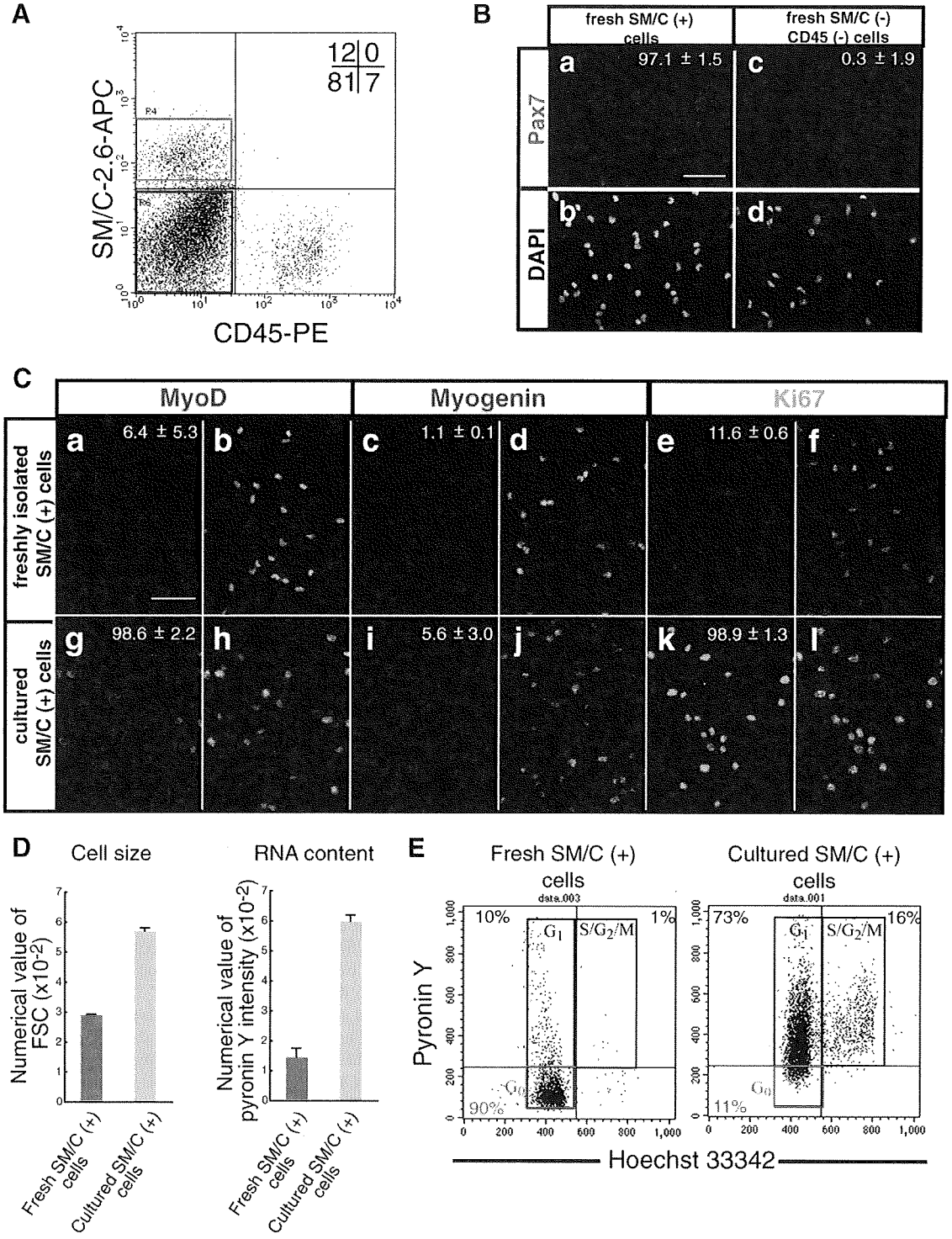

Figure 1. SM/C-2.6$^+$ cells isolated from skeletal muscle by fluorescence-activated cell sorting (FACS) are highly purified quiescent satellite cells and proliferate and express MyoD in culture. **(A):** Mononucleated cells prepared from uninjured limb muscles of adult mice were stained with anti-CD45 antibody and SM/C-2.6 monoclonal antibody. The SM/C-2.6$^+$ fraction (red square) and the SM/C-2.6$^-$/CD45$^-$ fraction (blue square) were collected for further analysis. **(B):** Freshly isolated SM/C-2.6$^+$ and SM/C-2.6$^-$/CD45$^-$ cells were stained with anti-Pax7 **(Ba, Bc)** antibody and DAPI **(Bb, Bd)**. The percentages of Pax7-positive cells in each cell fraction are shown. Cell fractionation was performed three times, and more than 300 cells from each fraction were counted. Scale bar: 50 μm. **(C):** Freshly isolated SM/C-2.6$^+$ cells and SM/C-2.6$^+$ cells cultured for 4 days in the presence of basic fibroblast growth factor were stained with antibodies to MyoD **(Ca, Cg)**, myogenin **(Cc, Ci)**, or Ki67 **(Ce, Ck)**. Percentages of MyoD-, myogenin-, or Ki67-positive cells are shown. Cell fractionation was performed three times, and more than 180 cells were counted each time. Nuclei were stained with DAPI **(Cb, Cd, Cf, Ch, Cj, Cl)**. Scale bar: 50 μm. **(D):** The mean value of FSC (cell size) and Pyronin Y intensity (RNA content) of freshly isolated SM/C-2.6$^+$ cells and satellite cells cultured in vitro. The value is an average of two independent experiments. **(E):** The percentages of cells in the G0 phase of the cell cycle were estimated by staining with Pyronin Y and Hoechst 33342. The number in the lower left of each FACS profile indicates the percentage of the G0 cells: 90% for fresh SM/C-2.6$^+$ cells and 11% for cultured SM/C-2.6$^+$ cells. Abbreviations: APC, allophycocyanin; DAPI, 4,6-diamidino-2-phenylindole; FSC, forward scatter; M, mitosis phase; PE, phycoerythrin; S, synthesis phase.

to be G0 cells [24]. Pyronin Y and Hoechst double staining shows that approximately 90% of fresh SM/C-2.6$^+$ cells were in the G0 phase of the cell cycle. In contrast, 90% of cultured SM/C-2.6$^+$ cells were cycling (Fig. 1E).

Thus, our procedure, which takes 5–6 hours in total to isolate 1–2 × 10^5 SM/C-2.6$^+$ cells from one C57BL/6 mouse, enables us to isolate satellite cells still in a quiescent and undifferentiated state. The yield corresponds to 10%–15% of the total mononucleated cells obtained from mouse hind limb muscles by enzymatic digestion. Therefore, in this report, we call freshly isolated SM/C-2.6$^+$ cells "quiescent satellite cells" and cultured, proliferating SM/C-2.6$^+$ cells "activated satellite cells." Our procedure was also applicable to dystrophin-deficient *mdx* muscle with modifications, although 30%–40% of *mdx* satellite cells are Ki67-positive (M. Ikemoto et al., submitted manuscript). Unfortunately, SM/C-2.6 did not react with satellite cells from dystrophin-deficient dystrophic dogs (data not shown).

Single Gene Analysis of Quiescent and Activated/Proliferating Satellite Cells

We prepared RNA samples from quiescent satellite cells and activated satellite cells and performed microarray analysis using Affymetrix GeneChips. Hybridization and data collection were performed four times using independent preparations of cells and RNA samples for each cell fraction. Raw data are available at http://www.ncbi.nlm.nih.gov/geo. The Gene Expression Omnibus accession number is GSE3483.

First, we compared the expression levels of individual genes in quiescent and activated states using GeneSpring software. We found that 507 genes (665 probes) were expressed in quiescent satellite cells at more than fivefold higher levels than in activated satellite cells (Fig. 2A). We roughly categorized these 507 genes into 11 gene groups: cell adhesion (15 genes), cell cycle regulation (26), proteolysis (21), cytoskeleton (13), cell surface (41), extracellular (61), immunoresponse (22), signal transduction (81), transcription (67), transport and metabolism (82), and unknown (78) based on Gene Ontology and listed all of them in supplemental online Table 1. On the other hand, 659 genes (814 probes) were upregulated (>fivefold) in the activated state (supplemental online Table 2). We also examined the gene expression of proliferating satellite cells/myoblasts in vivo that were directly isolated from regenerating muscle 2 days after cardiotoxin injection. The activated and proliferating satellite cells in vivo showed an expression profile quite similar to satellite cells cultured in vitro (data not shown).

Upregulation of Cell Cycle Regulators in Quiescent Satellite Cells

Under normal conditions, most satellite cells are in the G0 phase of the cell cycle, possibly preventing their premature exhaustion. It is of note that nine genes encoding negative regulators of the cell cycle were highly upregulated in the quiescent stage: *Rgs2* (*regulator of G-protein signaling 2*) (×69, ×23), *Rgs5* (×37, ×21), *Pmp22* (*peripheral myelin protein 22*)/*Gas3* (growth arrest specific 3) (×25), *Cdkn1c* (cyclin-dependent kinase inhibitor 1C)/*p57* (×14), *Spry1* (sprouty homolog 1) (×11), *Gas1* (×7, ×6), *Reck* (reversion-inducing-cysteine-rich protein with kazal motifs) (×6), *Ddit3* (DNA-damage inducible transcript 3) (×6), and *Trp63* (transformation-related protein 63) (×5) (supplemental online Table 1). Reverse transcription (RT)-PCR confirmed that *Rgs2*, *Pmp22*, *p57*, and *Spry1* are highly expressed in quiescent satellite cells and downregulated in activated satellite cells (Fig. 2Ba).

Cyclin-dependent kinase inhibitors (CKIs) play a key role in controlling the cell cycle in many cell types. p21 (CIP1) triggers the cell cycle exit of proliferating myoblasts to initiate myoblast terminal differentiation in response to differentiation signals [25]. p57 (KIP2) is induced in myoblasts upon differentiation. Gene targeting experiments showed that these two CKIs redundantly control cell cycle exit during myogenesis [26]. Compared with irreversible cell cycle arrest upon differentiation, however, attainment of a reversible G0 state by satellite cells is poorly understood. In vitro studies suggested that Rb family members p130 and p27 are involved in the reversible cell cycle exit of proliferating myoblasts to return satellite cells to quiescence [16]. In our experiments, p21 (×0.5), p27 (×1.5), and p130 (×2–3) were not significantly upregulated in quiescent satellite cells. Reflecting the levels of p57 mRNA, p57 protein was found in more than 90% of freshly isolated SM/C-2.6$^+$ cells (Fig. 2Ca). Whether p57 is required for acquisition and maintenance of quiescence of satellite cells remains to be determined in a future study.

Upregulation of Myogenic Inhibitors in Quiescent Satellite Cells

Quiescent satellite cells barely express myogenic basic helix-loop-helix (bHLH) factors. Activity of the *Myf-5* locus was revealed through a reporter gene, but Myf-5 protein is hardly detected in dormant satellite cells. On activation, satellite cells upregulate Myf5 and start to express MyoD [27] (Fig. 1). Our microarray analyses revealed that several myogenic inhibitory molecules were upregulated in quiescent satellite cells: *Bmp6* (*bone morphogenetic protein 6*) (×214), *Bmp4* (×66), *Bmp2* (×82), *Heyl* (*hairy/enhancer-of-split related with YRPW motif-like*)/*Herp3*/*Hrt3*/*hesr3* (×101, ×33, ×32), *Musculin*/*MyoR* (×83), *Notch3* (×9). Upregulation of *Bmp4*, *Bmp6*, *Msc*/*MyoR*, and *Heyl* in quiescent satellite cells was confirmed by RT-PCR (Fig. 2Bb). BMP4 is reported to negatively regulate MyoD expression in somite myogenesis [28] and differentiation of satellite cells, where BMP4-induced inhibition of myogenic differentiation requires Notch signaling [29]. Notch signaling is reported to inhibit the differentiation of myoblasts by repression of MyoD expression [30]. In postnatal muscle, Notch signaling controls satellite cell activation and their cell fate [31], and insufficient upregulation of the Notch ligand Delta is casually related to impaired regeneration of aged muscle [32]. Among several molecules in the Notch signaling pathway, our microarray analysis showed that *Notch3* and one of the Notch-effector genes, *Heyl*, are highly expressed in quiescent satellite cells. When cross-sections of normal mouse tibialis anterior (TA) muscle were stained with specific antibodies, HeyL was found in nearly all Pax7-positive nuclei, and Notch3 was expressed on the surface of mononuclear cells beneath the basal lamina (Fig. 2Cb, 2Cc). These results suggest that Notch3 and HeyL play roles in Notch signaling to inhibit muscle differentiation of satellite cells. Musculin/MyoR is a bHLH transcription factor originally cloned as a repressor of MyoD [33]. Musculin-null mice do not exhibit any skeletal muscle defect, but musculin is likely to negatively regulate MyoD in muscle regeneration [34].

In addition to negative regulators, two positive regulators of myogenesis, *Gli2* (*GLI-Kruppel family member GLI2*) (×29, ×13) and *Meox2* (*mesenchyme homeobox 2*) (×17), are preferentially expressed in quiescent satellite cells. Gli2 directly upregulates Myf5 [35], and Meox1 and 2 regulate Pax3 and Pax7 expressions [36]. These observations suggest that Gli2 and Meox2 maintain lineage identity in quiescent satellite cells.

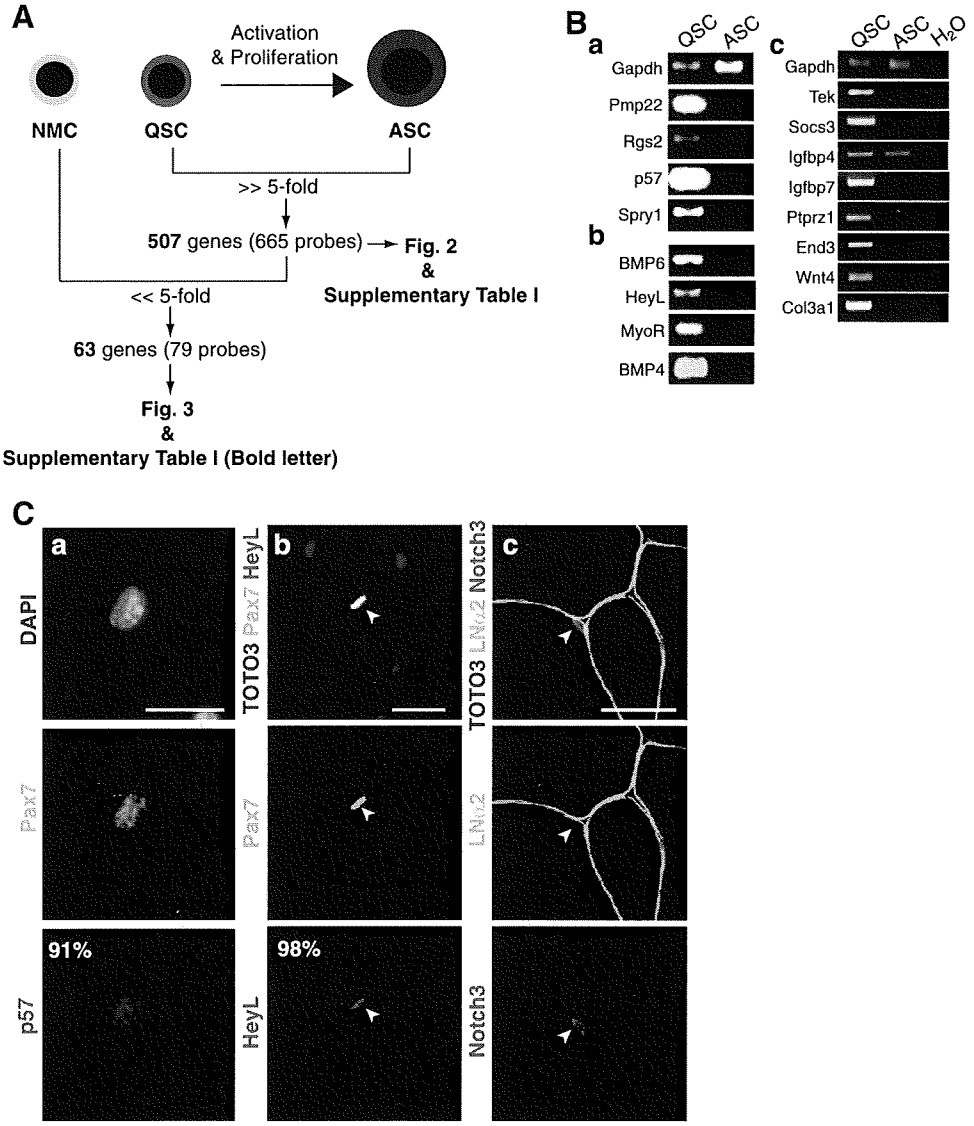

Figure 2. Identification of the genes expressed at higher levels in QSC than in ASC. **(A):** Outline of gene expression analysis at single gene level. Sixty-three genes out of 507 genes were found to be expressed at a higher level (more than fivefold) in quiescent satellite cells than in NMC. We applied Student's *t* test (*p* value .05) with multiple testing corrections (Benjamini and Hochberg false discovery rate). **(B):** Reverse transcription-polymerase chain reaction of eight relevant genes involved in cell cycle regulation **(Ba)**, inhibition of myogenesis **(Bb)**, or other biological process **(Bc)** (Table 1). Total RNAs were isolated from fluorescence-activated cell sorting-sorted SM/C-2.6$^+$ cells (QSC) and cultured SM/C-2.6$^+$ cells (ASC). *Gapdh* is control. **(Ca):** Mononucleated cells from intact skeletal muscle were stained with anti-p57 (red), Pax7 (green), and DAPI (blue) immediately after sorting. **(Cb, Cc):** Cross-sections of normal skeletal muscle were stained with antibodies to HeyL (red in **[Cb]**), Notch3 (red in **[Cc]**), Pax7 (green in **[Cb]**), or laminin α2 chain (green in **[Cc]**). More than 90% of Pax7-positive cells were positive for p57. Nearly all Pax7-positive cells expressed HeyL. Notch3 was expressed on the cell surface on satellite cells. Nuclei were stained with TOTO3 (blue). Scale bar: 20 μm. Abbreviations: ASC, activated satellite cells; DAPI, 4,6-diamidino-2-phenylindole; LNα2, laminin α2; NMC, nonmyogenic cells; QSC, quiescent satellite cells.

Identification of Quiescent Satellite Cell-Specific Genes

To identify quiescent satellite cell-specific genes from 507 genes (Fig. 2A), we next prepared RNA samples from nonmyogenic cells (SM/C-2.6$^-$/CD45$^-$ in Fig. 1A) and performed microarray analysis using Affymetrix GeneChips. Statistical analysis validated that 63 genes out of 507 genes were preferentially expressed (>fivefold) in quiescent satellite cells compared with nonmyogenic cells or activated satellite cells (genes in bold letters in supplemental online Table 1).

To confirm the microarray results, we next performed RT-PCR on 14 genes of interest. In addition to microarray samples, the results for TA muscle and a myogenic cell line, C2C12 cells, are also shown (Fig. 3). Two well-established satellite cell markers (Pax7 and M-cadherin) were expressed not only in quiescent satellite cells but also in activated satellite cells and/or C2C12 cells. In contrast, two cell surface molecules, Odz4, a mouse homolog of the *Drosophila* pair-rule gene *Odd Oz* [37], and CTR, a signaling molecule Tribbles1, and two extracellular molecules, endothelin3 and chordin-like2, were all confirmed to be expressed exclusively in quiescent satellite cells.

Gene Set Enrichment Analysis Revealed Gene Groups Upregulated in Quiescent Satellite Cells

Single-gene analysis permitted us to identify candidate genes that regulate quiescence and undifferentiated state of satellite cells in vivo. To complement the analysis at the single gene

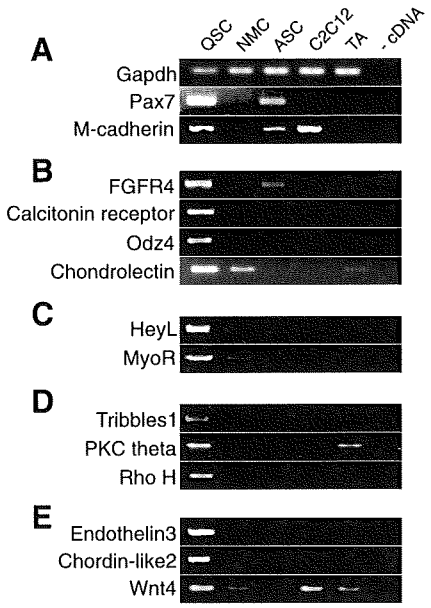

Figure 3. Reverse transcription-polymerase chain reaction (RT-PCR) of quiescent satellite cell-specific genes. Expression levels of quiescent satellite cell-specific genes in fluorescence-activated cell sorting-sorted SM/C-2.6$^+$ cells (lane 1), SM/C-2.6$^-$/CD45$^-$ nonmyogenic cells (lane 2), cultured SM/C-2.6$^+$ cells (lane 3), C2C12 cells (lane 4), and TA muscle (lane 5) were confirmed by RT-PCR. The genes are categorized into five groups: well-known satellite cell markers (**A**), cell surface receptors (**B**), transcription factors (**C**), signal molecules (**D**), and extracellular molecules (**E**). Lane 6 is the reaction without cDNA templates. Abbreviations: ASC, activated satellite cells; NMC, nonmyogenic cells; QSC, quiescent satellite cells; TA, tibialis anterior.

level, we performed gene set enrichment analysis [22]. GSEA is an analytical method that identifies small but coordinated changes of predefined gene sets but not up- or downregulation of individual genes, which therefore would help us to identify important signaling pathways or regulatory mechanisms for satellite cells. We used GO annotations [23] to group all genes on GeneChips and tried to extract gene sets that are upregulated as a whole in quiescent satellite cells compared with activated and proliferating satellite cells (Fig. 4). When all genes were categorized into 1,674 gene sets according to their biological process ontology, only three gene sets were judged to be coordinately upregulated in quiescent satellite cells (FDR $<$ 0.25): cell-cell adhesion, regulation of cell growth, and transmembrane receptor protein tyrosine phosphatase signaling pathway (Table 1). When all genes were grouped into 1,698 gene sets according to cellular component ontology, three gene sets, insoluble fraction, extracellular region, and collagens, were found to be coordinately upregulated in quiescent satellite cells compared with activated/proliferating satellite cells (Table 1). When grouped into 412 gene sets based on their predicted molecular functions, three gene sets, extracellular matrix structural constituent conferring tensile strength, copper ion binding, and lipid transporter activity, were found to be coordinately upregulated in quiescent satellite cells (Table 1). Seven genes listed in Table 1 (*Tek, Socs3, Igfbp7, Ptprz1, End3, Wnt4,* and *Col3a1*) were confirmed to be upregulated in quiescent satellite cells by RT-PCR (Fig. 2Bc). A more detailed discussion on GSEA results is in the supplemental online Discussion.

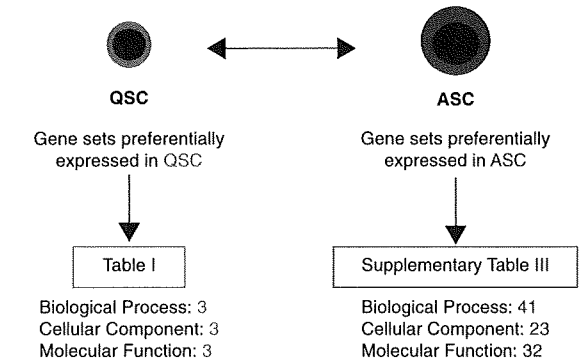

Figure 4. Gene set enrichment analysis (GSEA) of quiescent and activated satellite cells. Summary of GSEA comparing QSC with ASC using gene sets based on three major Gene Ontology trees: cellular component, biological process, and molecular function. Gene sets with high enrichment score (1 − [false discovery rate q value] are $>$0.75) are listed in Table 1 and supplemental online Table 3. Abbreviations: ASC, activated satellite cells; QSC, quiescent satellite cells.

Gene Sets That Are Coordinately Upregulated upon Activation

Many gene sets were found to be coordinately upregulated in activated/proliferating satellite cells compared with quiescent satellite cells (Fig. 4). These are involved in active synthesis of DNA, RNA and protein, progression of cell cycle (*Cdc2a, Cdc20, Cdc25c, Ccnb1, Ccna2,* etc.), mitochondrial activities, and so on. The gene sets are all listed in supplemental online Table 3. The results well reflect active cell cycling and high metabolic activity of satellite cells.

Expression of Cell-Cell Adhesion Molecules on Satellite Cells

Both single gene analysis and GSEA suggest that cell-cell adhesion is one of the key elements in the regulation of satellite cells. Preferential expression of the following genes in quiescent satellite cells was confirmed by RT-PCR and quantitative PCR (supplemental online Fig. 1A, 1B): *VE-cadherin* (*cadherin 5*), *Vcam1*, *Icam1*, *Cldn5* (*claudin 5*), *Esam* (*endothelial cell-specific adhesion molecule*), and *Pcdhb9* (*protocadherin beta 9*). To date, several cell surface markers for satellite cells have been identified, including M-cadherin, syndecan3, syndecan4, c-met, Vcam-1, NCAM-1, and CD34 [5, 38–43]. Vascular endothelial (VE)-cadherin, Icam1, claudin5, Esam, and Pcdhb9 should be added to the list. Because *Esam* is upregulated in long-term hematopoietic stem cells and mammary gland side population cells [44, 45], the expression of *Esam* in quiescent satellite cells is quite intriguing. When transverse sections of adult skeletal muscle were stained with specific antibodies, M-cadherin was found at the site of contact between satellite cells and myofibers (supplemental online Fig. 1C) [38]. Vcam-1 and VE-cadherin proteins are also detected at the boundary of satellite cells and myofibers. Although their roles in regulation of satellite cells remain to be determined, our observations suggest that cell-cell adhesion molecules have critical roles in keeping satellite cells in an undifferentiated and quiescent state and in protecting satellite cells from cell death. We also confirmed that FACS with Vcam-1 anti-

Table 1. Gene sets upregulated in quiescent satellite cells and genes with high enrichment scores

	1 − (FDR q value)
Biological process	
Cell-cell adhesion	.791
Tek, Vcam1, Icam2, Cldn5, Cdh5, Icam1	
Regulation of cell growth	.787
Socs3, Htra1, Htra3, Ctgf, Igfbp4, Creg1, Igfbp7, Epc1, Cyr61, Crim1, Nov, Igfbp6, Nedd9	
Transmembrane receptor protein tyrosine phosphatase signaling pathway	.751
Ptprz1, Ptprf, Ptprb, Ptprd, Ptprk, Ptprs, Ptprr	
Cellular component	
Insoluble fraction	.786
Dmd, Dag1, Plec1, Des, Hspb1	
Extracellular region	.766
Sepp1, Htra1, Edn3, Cxcl1, Loxl1, Htra3, Thbs4, Ctgf, Ntf3, Twsg1, Ccl27, Rarres2, Ltbp3, Igfbp4, Apoe, Igf1, Ibsp, Trf, Pthlh, Polydom, Ccl11, Abca3, Thbs3, Wnt4, Pros1, Vwa1, Comp, Nppc, Cyp4v3, Ccl19, Nts, Fbln2, Cocoacrisp, Cxcl2, Igfbp7, C1r, Thbs2, Ccl6, Calca, Cyr61, Icosl, Ccl21c, Crim1, Il6, Degb10, Cxcl9, Csng, C3, Cxcl10, Cxcl14, Inhbb, Il15, Nov, Igfbp6, Mglap, Dkk2, Tnfsf12, Ifnb1, Tfpi2, Cxcl11, Il18, Pi16, Pycard, Lzp-s, Stc1, Lyzs	
Collagen	.766
Col3a1, Col6a2, Col17a1, Col1a2, Col15a1, Col6a3, Col5a3, Col1a1, Col4a1, Col5a1, Col11a1	
Molecular function	
Extracellular matrix structural constituents conferring tensile strength	.774
Col3a1, Col6a2, Col17a1, Col1a2, Col15a1, Col6a3, Col16a1, Col1a1, Col4a1, Col4a5, Col5a1, Col11a1, Col11a2, Col9a1, Col4a2, Col4a4	
Copper ion binding	.764
Aoc3, Cp, Loxl1, Mt1, Atp7a, Heph, Loxl2, Nr1h3	
Lipid transporter activity	.752
Vldlr, Lp1, Apoe, Sorl1, Ldlr, Gpld1, Lrp1	

Gene names are listed according to the rank of enrichment scores. Underlined genes (46/118 genes) are also listed in supplemental online Table 1.
Abbreviation: FDR, false discovery rate.

body efficiently enriches quiescent satellite cells as SM/C-2.6 does (supplemental online Fig. 2).

Calcitonin Receptor Is Sharply Downregulated on Activated Satellite Cells and Reappeared on Renewed Satellite Cells During Muscle Regeneration

RT-PCR verified that CTR is exclusively expressed in quiescent satellite cells but not in activated satellite cells or in nonmyogenic cells (Fig. 3). In addition, we confirmed that calcitonin mRNA is expressed in satellite cells (data not shown). Therefore, we examined the expression of CTR protein in vivo using immunohistochemistry. As shown in Figure 5A, CTR protein was observed in Pax7-positive mononuclear cells beneath the basal lamina in uninjured muscle. We next stained cross-sections of regenerating muscle with anti-CTR antibody. Three days after cardiotoxin injection, many activated satellite cells were stained with anti-M-cadherin antibodies, but CTR expression was not detected on activated satellite cells on the serial sections (Fig. 5B). Furthermore, there were no $Pax7^+/CTR^+$ cells on muscle sections until 7 days after injury (cardiotoxin [CTX]-7d), when $Pax7^+/CTR^+$ cells were again found at the periphery of centrally nucleated, relatively large myofibers but not of small regenerating fibers (Fig. 5C, 5D). The number of $Pax7^+/CTR^+$ cells gradually increased thereafter and reached the level of uninjured muscle by CTX-14d (Fig. 5D). Interestingly, approximately 20% of $Pax7^+/CTR^+$ cells on CTX-7d were found outside the basal lamina (Fig. 5E). This atypical position of satellite cells was transient, and the ratio of satellite cells residing beneath the basal lamina increased during myofiber maturation (data not shown). Taken together, the results suggest that the expression of CTR is found not only on quiescent satellite cells but also on newly formed satellite cells that are closely associated with maturing myofibers.

Calcitonin Inhibits Activation of Quiescent Satellite Cells

To investigate the roles of CTR in the regulation of satellite cells, eel calcitonin, elcatonin, was added to the culture of quiescent satellite cells in vitro before or after activation. Addition of calcitonin before activation significantly inhibited BrdU uptake by quiescent satellite cells (Fig. 6A) but not by already activated satellite cells (Fig. 6A). Interestingly, a short exposure (0.5 hours) to calcitonin was enough to suppress the activation of quiescent satellite cells (Fig. 6B).

MyoD staining of satellite cells revealed that calcitonin/CTR signaling delays the induction of MyoD in quiescent satellite cells (Fig. 6C). The lower percentage of Ki67-positive cells in calcitonin-treated satellite cells also indicated that calcitonin delays the entry of quiescent satellite cells into the cell cycle (Fig. 6C). Calcitonin-treated cells were considerably smaller than control cells on the second day of culture (Fig. 6D), again indicating delayed activation of satellite cells in the presence of calcitonin. A terminal deoxynucleotidyl transferase dUTP nick-end labeling assay excludes the possibility that calcitonin induced apoptosis in satellite cells (Fig. 6E).

To further investigate the effects of calcitonin on activation of quiescent satellite cells, we prepared living single muscle fibers from mouse extensor digitorum longus muscles by using the collagenase digestion method [20] and plated them onto Matrigel-coated 24-well plates at a density of one fiber per well in the presence or absence of calcitonin. In control wells, many satellite cells had detached and migrated from the myofibers 2 days after plating (Fig. 6F). Calcitonin significantly reduced the numbers of satellite cells that had detached from myofibers (Fig. 6F). It was reported that

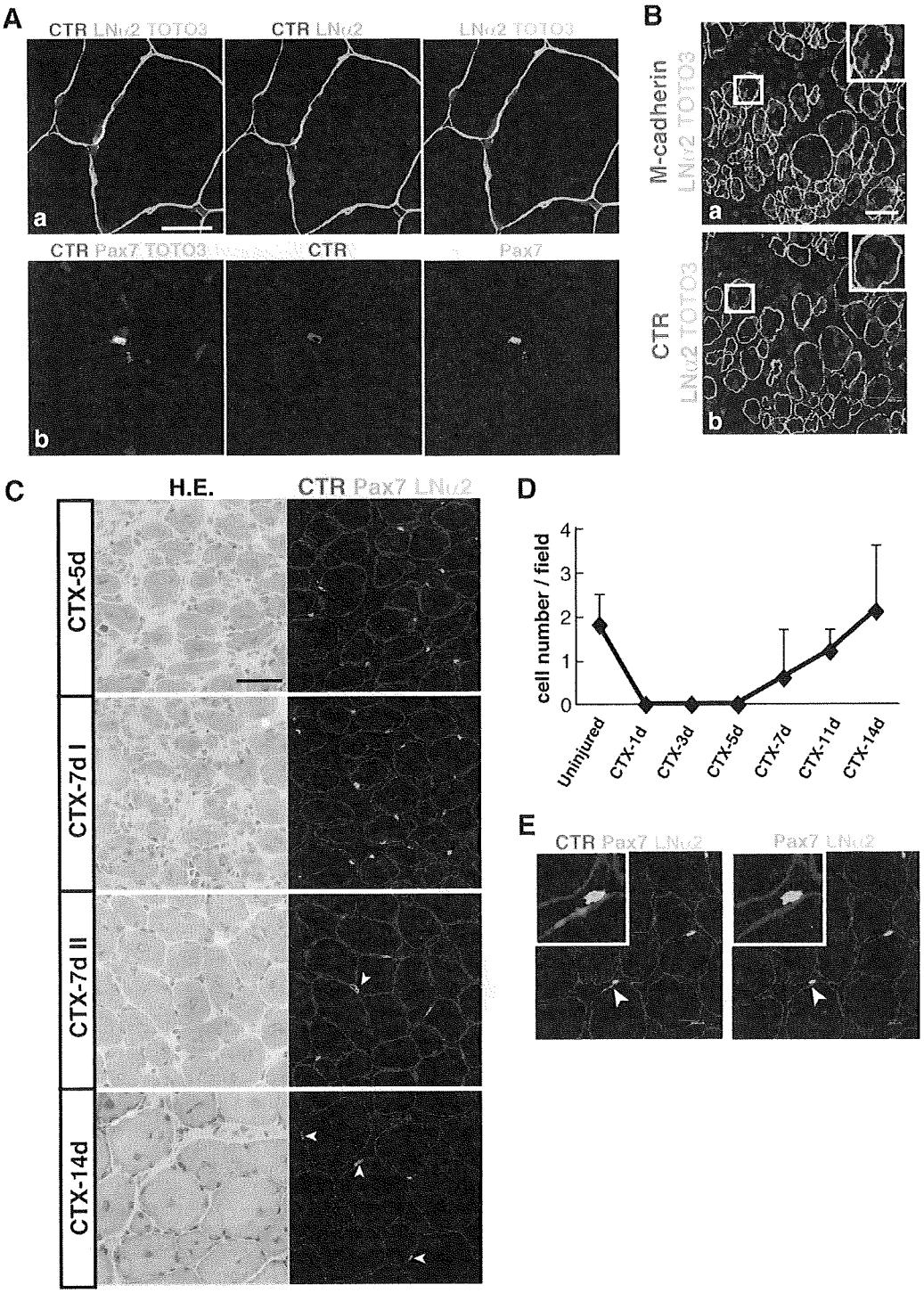

Figure 5. Reappearance of CTR- and Pax7-positive satellite cells in regenerating muscle 7 days after cardiotoxin injection. **(A):** Cross-sections of uninjured skeletal muscle were stained with antibodies to calcitonin receptor (red), laminin α2 chain (green in [Aa]), or Pax7 (green in [Ab]). Nuclei were stained with TOTO3 (blue). Scale bar: 20 μm. **(B):** Three days after CTX injection, regenerating muscles were dissected, and serial cross-sections were stained with antibodies to M-cadherin (red in **[Ba]**) or CTR (red in **[Bb]**) and anti-laminin α2 (green in **[Ba, Bb]**) antibodies. Insets show close-ups of marked areas by white squares. Nuclei were stained with TOTO3 (blue). Scale bar: 40 μm. **(C):** Tibialis anterior muscles were sampled at five (CTX-5d), seven (CTX-7d), and 14 days (CTX-14d) after CTX injection. Sections were coimmunostained with anti-CTR (red), Pax7 (green), and laminin α2 chain (blue) antibodies. Serial sections were stained with H.E. Note that $Pax7^+/CTR^+$ cells were first detected on the seventh day of regeneration around regenerating muscle fibers with a large diameter (CTX-7d II) but not around small-sized fibers (CTX-7d I). Arrowheads indicate CTR-positive Pax7-positive cells. Scale bar: 40 μm. **(D):** Numbers of $Pax7^+/CTR^+$ cells per field at 1, 3, 5, 7, 11, and 14 days after CTX injection. $Pax7^+/CTR^+$ cells were counted in 12–21 randomly selected fields in the regenerating area. The average is shown with SD. **(E):** Cross-sections of regenerating muscle 7 days after CTX injection were coimmunostained with CTR (red), Pax7 (green), and laminin α2 (blue). A typical $Pax7^+/CTR^+$ satellite cell outside the basal lamina is shown (arrowheads). Scale bar: 20 μm. Abbreviations: CTR, calcitonin receptor; CTX, cardiotoxin; d, day; H.E., hematoxylin and eosin; LNα2, laminin α2.

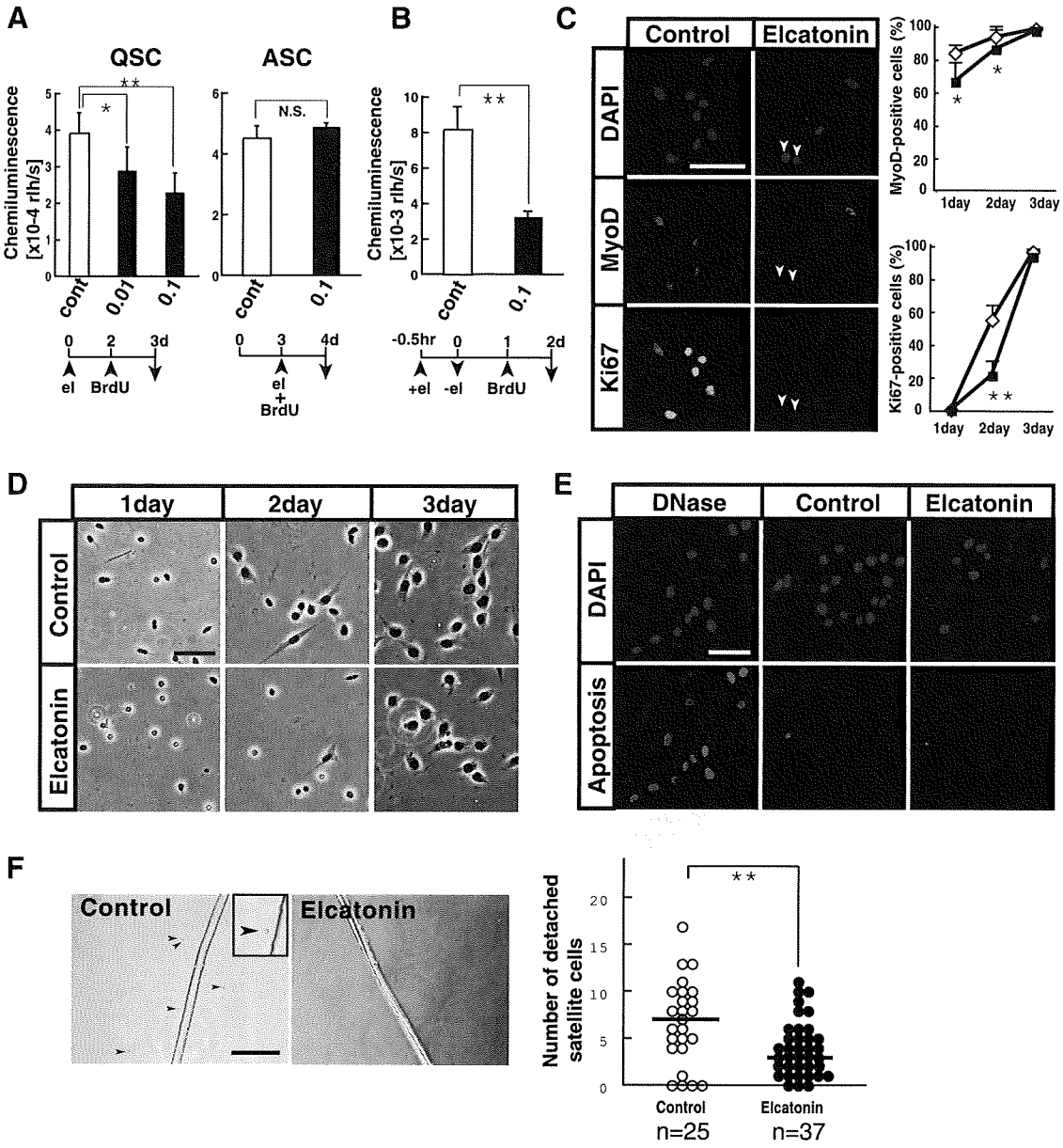

Figure 6. Calcitonin receptor agonist, elcatonin, suppresses activation of quiescent satellite cells. **(A):** Freshly isolated SM/C-2.6$^+$ cells (QSC) and cultured SM/C-2.6$^+$ cells (ASC) were grown in the presence (black) or absence (white) of eel calcitonin, elcatonin. Left: QSC were cultured for 2 days with (0.01 U/ml or 0.1 U/ml) or without elcatonin and then cultured for an additional 24 hours in the presence of BrdU. Right: QSC were cultured for 3 days and then cultured for 24 hours in the presence or absence of elcatonin and BrdU. The vertical axis shows the mean BrdU uptake by satellite cells of three experiments with SD; * $p < .05$, ** $p < .01$ (analysis of variance [ANOVA] test). **(B):** BrdU uptake by QSC exposed to elcatonin for 30 minutes prior to plating. Values are means with SD ($n = 3$); ** $p < .01$. **(C):** QSC cultured in the presence or absence of 0.1 U/ml elcatonin for 2 days were stained with anti-MyoD (red) or Ki67 (green) antibodies. Nuclei were stained with DAPI (blue). Arrowheads indicate MyoD- and Ki67-negative satellite cells. Graphs show the frequency of MyoD- or Ki67-positive cells 1, 2, or 3 days after plating with (closed square) or without (open diamond) elcatonin. More than 100 cells were counted. Values are means with SD; * $p < .05$, ** $p < .01$. Scale bar: 50 μm. **(D):** Phase contrast images of satellite cells 1, 2, and 3 days after plating in the presence or absence of 0.1 U/ml elcatonin. Note that many elcatonin-treated satellite cells are smaller than nontreated cells 2 days after plating. Scale bar: 50 μm. **(E):** Terminal deoxynucleotidyl transferase dUTP nick-end labeling assay on satellite cells cultured with or without elcatonin for 2 days. Apoptotic cells are in red. Nuclei were stained with DAPI (blue). As a positive control, satellite cells were pretreated with DNase. Scale bar: 50 μm. **(F):** Activation of satellite cells on myofibers in vitro. Isolated muscle fibers were plated at a density of one fiber per well and cultured with or without elcatonin (0.1 U/ml) for 2 days, and the numbers of satellite cells that had detached and migrated from each muscle fiber (arrowheads) were counted. Inset is a close-up image of a detached satellite cell. Scale bar: 100 μm. ANOVA t test, ** $p < .01$. Abbreviations: ASC, activated satellite cells; BrdU, 5-bromo-2′-deoxyuridine; d, days; DAPI, 4,6-diamidino-2-phenylindole; el, elcatonin; hr, hours; NS, nonsignificant; QSC, quiescent satellite cells.

calcitonin signaling was mediated via cAMP [46]. An analog of cAMP, dibutyryl cAMP, and an activator of adenylate cyclase, forskolin, also attenuated the activation of satellite cells in vitro (data not shown). Collectively, our results suggest that calcitonin/CTR signaling inhibits activation of satellite cells but not their proliferation or survival. The downstream target molecules of calcitonin/CTR remain to be determined.

CONCLUSION

Single gene-level analysis revealed several candidate genes that negatively regulate cell cycling of satellite cells. Furthermore, our results suggested that satellite cells express both myogenic and antimyogenic molecules to maintain their delicate state.

GSEA showed that dormant satellite cells coordinately express gene groups involved in cell-cell adhesion, cell-extracellular matrix interaction, copper and iron homeostasis, lipid transport, and regulation of cell growth. Although the result shows one aspect of regulation of quiescent satellite cells, more elaborate gene grouping might be needed to further understand the molecular regulation of quiescent satellite cells.

Finally, we showed that calcitonin receptor is specifically expressed on quiescent satellite cells and transmits signals that attenuate the entry of quiescent satellite cells into the cell cycle. Our results would greatly facilitate the investigation of molecular regulation of satellite cells in both physiological and pathological conditions.

ACKNOWLEDGMENTS

This work was supported by Grants for Research on Nervous and Mental Disorders (16B-2), Health Science Research Grants for Research on the Human Genome and Gene Therapy (H16-genome-003), for Research on Brain Science (H15-Brain-021) from the Japanese Ministry of Health, Labor and Welfare, Grants-in-Aids for Scientific Research (14657158, 153,90281, and 165,90333) from the Japanese Ministry of Education, Culture, Sports, Science and Technology, and "Ground-Based Research Program for Space Utilization" promoted by Japan Space Forum.

DISCLOSURE OF POTENTIAL CONFLICTS OF INTEREST

The authors indicate no potential conflicts of interest.

REFERENCES

1 Bischoff R. Analysis of muscle regeneration using single myofibers in culture. Med Sci Sports Exerc 1989;21(suppl 5):S164–S172.
2 Partridge T. Reenthronement of the muscle satellite cell. Cell 2004;119: 447–448.
3 Mauro A. Satellite cell of skeletal muscle fibers. J Biophys Biochem Cytol 1961;9:493–495.
4 Schultz E, Gibson MC, Champion T. Satellite cells are mitotically quiescent in mature mouse muscle: an EM and radioautographic study. J Exp Zool 1978;206:451–456.
5 Cornelison DD, Wold BJ. Single-cell analysis of regulatory gene expression in quiescent and activated mouse skeletal muscle satellite cells. Dev Biol 1997;191:270–283.
6 Bischoff R. Satellite and stem cells in muscle regeneration. In: Engel AG, Franzini-Armstrong C, eds. Myology. Vol 1. New York: McGraw-Hill, 2004:66–86.
7 Collins CA, Olsen I, Zammit PS et al. Stem cell function, self-renewal, and behavioral heterogeneity of cells from the adult muscle satellite cell niche. Cell 2005;122:289–301.
8 Seale P, Sabourin LA, Girgis-Gabardo A et al. Pax7 is required for the specification of myogenic satellite cells. Cell 2000;102:777–786.
9 Grounds MD, Yablonka-Reuveni Z. Molecular and cell biology of skeletal muscle regeneration. Mol Cell Biol Hum Dis Ser 1993;3: 210–256.
10 Wagers AJ, Conboy IM. Cellular and molecular signatures of muscle regeneration: Current concepts and controversies in adult myogenesis. Cell 2005;122:659–667.
11 Asakura A, Komaki M, Rudnicki M. Muscle satellite cells are multipotential stem cells that exhibit myogenic, osteogenic, and adipogenic differentiation. Differentiation 2001;68:245–253.
12 Wada MR, Inagawa-Ogashiwa M, Shimizu S et al. Generation of different fates from multipotent muscle stem cells. Development 2002;129: 2987–2995.
13 Shefer G, Wleklinski-Lee M, Yablonka-Reuveni Z. Skeletal muscle satellite cells can spontaneously enter an alternative mesenchymal pathway. J Cell Sci 2004;117:5393–5404.
14 McCroskery S, Thomas M, Maxwell L et al. Myostatin negatively regulates satellite cell activation and self-renewal. J Cell Biol 2003;162: 1135–1147.
15 Thomas M, Langley B, Berry C et al. Myostatin, a negative regulator of muscle growth, functions by inhibiting myoblast proliferation. J Biol Chem 2000;275:40235–40243.
16 Cao Y, Zhao Z, Gruszczynska-Biegala J et al. Role of metalloprotease disintegrin ADAM12 in determination of quiescent reserve cells during myogenic differentiation in vitro. Mol Cell Biol 2003;23: 6725–6738.
17 Carnac G, Fajas L, L'Honore A et al. The retinoblastoma-like protein p130 is involved in the determination of reserve cells in differentiating myoblasts. Curr Biol 2000;10:543–546.
18 Fukada S, Higuchi S, Segawa M et al. Purification and cell-surface marker characterization of quiescent satellite cells from murine skeletal muscle by a novel monoclonal antibody. Exp Cell Res 2004;296: 245–255.
19 Uezumi A, Ojima K, Fukada S et al. Functional heterogeneity of side population cells in skeletal muscle. Biochem Biophys Res Commun 2006;341:864–873.
20 Rosenblatt JD, Lunt AI, Parry DJ et al. Culturing satellite cells from living single muscle fiber explants. In Vitro Cell Dev Biol Anim 1995; 31:773–779.
21 Ojima K, Uezumi A, Miyoshi H et al. Mac-1(low) early myeloid cells in the bone marrow-derived SP fraction migrate into injured skeletal muscle and participate in muscle regeneration. Biochem Biophys Res Commun 2004;321:1050–1061.
22 Mootha VK, Lindgren CM, Eriksson KF et al. PGC-1alpha-responsive genes involved in oxidative phosphorylation are coordinately downregulated in human diabetes. Nat Genet 2003;34:267–273.
23 Ashburner M, Ball CA, Blake JA et al. Gene ontology: Tool for the unification of biology. The Gene Ontology Consortium. Nat Genet 2000;25:25–29.
24 Holyoake T, Jiang X, Eaves C et al. Isolation of a highly quiescent subpopulation of primitive leukemic cells in chronic myeloid leukemia. Blood 1999;94:2056–2064.
25 Missero C, Calautti E, Eckner R et al. Involvement of the cell-cycle inhibitor Cip1/WAF1 and the E1A-associated p300 protein in terminal differentiation. Proc Natl Acad Sci U S A 1995;92:5451–5455.
26 Zhang P, Wong C, Liu D et al. p21(CIP1) and p57(KIP2) control muscle differentiation at the myogenin step. Genes Dev 1999;13:213–224.
27 Cooper RN, Tajbakhsh S, Mouly V et al. In vivo satellite cell activation via Myf5 and MyoD in regenerating mouse skeletal muscle. J Cell Sci 1999;112:2895–2901.
28 Reshef R, Maroto M, Lassar AB. Regulation of dorsal somitic cell fates: BMPs and Noggin control the timing and pattern of myogenic regulator expression. Genes Dev 1998;12:290–303.
29 Dahlqvist C, Blokzijl A, Chapman G et al. Functional Notch signaling is required for BMP4-induced inhibition of myogenic differentiation. Development 2003;130:6089–6099.
30 Kuroda K, Tani S, Tamura K et al. Delta-induced Notch signaling mediated by RBP-J inhibits MyoD expression and myogenesis. J Biol Chem 1999;274:7238–7244.
31 Conboy IM, Rando TA. The regulation of Notch signaling controls satellite cell activation and cell fate determination in postnatal myogenesis. Dev Cell 2002;3:397–409.
32 Conboy IM, Conboy MJ, Smythe GM et al. Notch-mediated restoration of regenerative potential to aged muscle. Science 2003;302: 1575–1577.
33 Lu J, Webb R, Richardson JA et al. MyoR: A muscle-restricted basic helix-loop-helix transcription factor that antagonizes the actions of MyoD. Proc Natl Acad Sci U S A 1999;96:552–557.
34 Zhao P, Hoffman EP. Musculin isoforms and repression of MyoD in muscle regeneration. Biochem Biophys Res Commun 2006;342: 835–842.
35 Gustafsson MK, Pan H, Pinney DF et al. Myf5 is a direct target of long-range Shh signaling and Gli regulation for muscle specification. Genes Dev 2002;16:114–126.
36 Mankoo BS, Skuntz S, Harrigan I et al. The concerted action of Meox homeobox genes is required upstream of genetic pathways essential for the formation, patterning and differentiation of somites. Development 2003;130:4655–4664.

37 Zhou XH, Brandau O, Feng K et al. The murine Ten-m/Odz genes show distinct but overlapping expression patterns during development and in adult brain. Gene Expr Patterns 2003;3:397–405.
38 Irintchev A, Zeschnigk M, Starzinski-Powitz A et al. Expression pattern of M-cadherin in normal, denervated, and regenerating mouse muscles. Dev Dyn 1994;199:326–337.
39 Cornelison DD, Filla MS, Stanley HM et al. Syndecan-3 and syndecan-4 specifically mark skeletal muscle satellite cells and are implicated in satellite cell maintenance and muscle regeneration. Dev Biol 2001;239: 79–94.
40 Beauchamp JR, Heslop L, Yu DS et al. Expression of CD34 and Myf5 defines the majority of quiescent adult skeletal muscle satellite cells. J Cell Biol 2000;151:1221–1234.
41 Jesse TL, LaChance R, Iademarco MF et al. Interferon regulatory factor-2 is a transcriptional activator in muscle where It regulates expression of vascular cell adhesion molecule-1. J Cell Biol 1998; 140:1265–1276.
42 Illa I, Leon-Monzon M, Dalakas MC. Regenerating and denervated human muscle fibers and satellite cells express neural cell adhesion molecule recognized by monoclonal antibodies to natural killer cells. Ann Neurol 1992;31:46–52.
43 Charge SB, Rudnicki MA. Cellular and molecular regulation of muscle regeneration. Physiol Rev 2004;84:209–238.
44 Forsberg EC, Prohaska SS, Katzman S et al. Differential expression of novel potential regulators in hematopoietic stem cells. PLoS Genet 2005;1:e28.
45 Behbod F, Xian W, Shaw CA et al. Transcriptional profiling of mammary gland side population cells. STEM CELLS 2006;24:1065–1074.
46 Becker K, Muller B, Nylen E et al. Calcitonin Gene Family of Peptides. Vol 1. 2nd ed. New York: Academic Press, 2002.

See www.StemCells.com for supplemental material available online.

EXPERIMENTAL CELL RESEARCH 314 (2008) 387–397

available at www.sciencedirect.com

ScienceDirect

www.elsevier.com/locate/yexcr

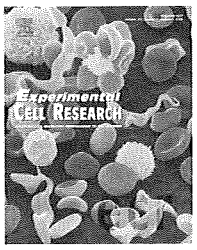

Research Article

Localized cyclic AMP-dependent protein kinase activity is required for myogenic cell fusion

*Atsushi Mukai, Naohiro Hashimoto**

Department of Regenerative Medicine, National Institute for Longevity Sciences, National Center for Geriatrics and Gerontology, 36-3 Gengo, Morioka, Oobu, Aichi 474-8522, Japan

ARTICLE INFORMATION

Article Chronology:
Received 11 August 2007
Revised version received
7 October 2007
Accepted 10 October 2007
Available online 17 October 2007

Keywords:
Myogenesis
Cell fusion
Myotube
Myoblast
Muscle
Terminal differentiation
Lamellipodium

ABSTRACT

Multinucleated myotubes are formed by fusion of mononucleated myogenic progenitor cells (myoblasts) during terminal skeletal muscle differentiation. In addition, myoblasts fuse with myotubes, but terminally differentiated myotubes have not been shown to fuse with each other. We show here that an adenylate cyclase activator, forskolin, and other reagents that elevate intracellular cyclic AMP (cAMP) levels induced cell fusion between small bipolar myotubes in vitro. Then an extra-large myotube, designated a "myosheet," was produced by both primary and established mouse myogenic cells. Myotube-to-myotube fusion always occurred between the leading edge of lamellipodia at the polar end of one myotube and the lateral plasma membrane of the other. Forskolin enhanced the formation of lamellipodia where cAMP-dependent protein kinase (PKA) was accumulated. Blocking enzymatic activity or anchoring of PKA suppressed forskolin-enhanced lamellipodium formation and prevented fusion of multinucleated myotubes. Localized PKA activity was also required for fusion of mononucleated myoblasts. The present results suggest that localized PKA plays a pivotal role in the early steps of myogenic cell fusion, such as cell-to-cell contact/recognition through lamellipodium formation. Furthermore, the localized cAMP–PKA pathway might be involved in the specification of the fusion-competent areas of the plasma membrane in lamellipodia of myogenic cells.

Introduction

Skeletal muscle fibers are multinucleated, non-mitotic cells. This unique cell type is derived from multinucleated myotubes, which are formed by the fusion of mononucleated myogenic progenitor cells (myoblasts). Myoblasts fuse to each other or to existing myofibers during both development and repair of skeletal muscle. Myoblast fusion is cell-specific because myoblasts do not fuse with non-myogenic cells [1]. Myoblast fusion consists of a series of steps such as myoblast–myoblast contact, recognition, adhesion, and plasma membrane breakdown/union [2]. However, little is known about the molecular mechanisms that regulate cell fusion during muscle development and regeneration.

The genes essential to myotube formation have been identified in *Drosophila*. They encode proteins that mediate a particular step of myoblast fusion [3,4]. In contrast to the detailed knowledge of the molecules involved in muscle cell fusion in *Drosophila*, the molecular mechanisms that control each step of myogenic cell fusion in mammals remain to be resolved, although a number of molecules have been implicated in regulating muscle fiber formation. Extracellular matrix receptor integrins and adhesion molecules such as cadherins, NCAM, CD9, CD81, and ADAMs may contribute to the regulation of the

* *Corresponding author.*
E-mail address: nao@nils.go.jp (N. Hashimoto).

0014-4827/$ – see front matter © 2007 Elsevier Inc. All rights reserved.
doi:10.1016/j.yexcr.2007.10.006

steps of recognition and adhesion in myoblast fusion [5,6]. However, how they coordinate their functions in the recognition/adhesion steps prior to plasma membrane fusion remains puzzling. In addition, few molecules involved in the regulation of plasma membrane fusion have been identified, although many membrane molecules have been implicated in myoblast fusion. One of these is cholesterol. It is involved in maintaining membrane fluidity and the structure of lipid microdomains. Membrane fusion takes place within the cholesterol-free areas of the myoblast plasma membrane [7]. However, the role of cholesterol in muscle cell fusion is not well understood because inconsistent results have been reported [8,9]. Because an increase of membrane fluidity is assumed to be required for plasma membrane fusion, the concentration of membrane cholesterol in myoblasts should decrease prior to membrane fusion. Therefore, the molecular mechanisms that regulate the distribution of membrane cholesterol and other membrane molecules at the fusion-competent areas of the plasma membrane should be identified. Unfortunately, the fusion-competent area of a membrane prior to myoblast fusion has not been positively identified.

To identify the key molecules that render an area of plasma membrane fusion-competent, we determined the stimulus and culture conditions that enhance or suppress muscle cell fusion in vitro. In contrast to mononucleated myoblasts, it has been unclear whether myotubes fuse together in vitro and in vivo. However, we found here that several reagents, such as forskolin, which elevate intracellular cyclic AMP (cAMP) levels, induce fusion between myotubes. The results suggest that the localized cAMP-dependent protein kinase (PKA) activity plays a critical role in the specification of fusion-competent areas of the plasma membrane.

Materials and methods

Cell culture

The mouse myogenic cell clone Ric10 was established from multiclonal myogenic cells derived from muscle satellite cells in the normal gastrocnemius muscle of an adult female ICR mouse [10]. Ric10 cells were plated on dishes coated with type I collagen (Sumilon, Tokyo, Japan) and cultured at 37 °C under 10% CO_2 in primary cultured myocyte growth medium (pmGM) consisting of Dulbecco's modified Eagle's medium (DMEM) supplemented with 20% fetal bovine serum (FBS), 2% Ultroser G (Biosepra, Cedex-Saint-Christophe, France), and glucose (4.5 mg ml^{-1}). For induction of myogenic differentiation, 2×10^4 of the cells were replated on a 35-mm dish and cultured in primary cultured myocyte differentiation medium (pmDM) consisting of the chemically defined medium TIS [11,12] supplemented with 2% FBS.

COM3 cells were isolated from the mouse myoblastic cell line C2C12 and maintained in medium consisting of DMEM supplemented with 10% FBS and glucose (4.5 mg ml^{-1}) [13]. For induction of myogenic differentiation, 5×10^4 of COM3 cells were plated on a 35-mm dish, and then the medium was switched to TIS on the next day.

Primary cultured mouse myogenic progenitor cells were isolated from gastrocnemius muscles of adult C57BL/6J mice and cultured in pmGM as described previously [10,14].

Immunofluorescence and immunocytochemical analyses

Cells were grown on collagen-coated culture dishes for immunofluorescence and immunocytochemical analysis. The cultured cells were fixed with 4% paraformaldehyde for 10 min at room temperature or on ice, and then permeabilized in phosphate buffered saline (PBS) supplemented with 0.5% Triton X-100 and 1% donkey serum for 20 min. Then the cells were incubated for 12 to 36 h at 4 °C with a mouse monoclonal antibody to sarcomeric myosin heavy chain (undiluted culture supernatant; MyHC) [15] or a goat polyclonal antibody to cAMP-dependent protein kinase type II subunit (RII) (1:100 dilution; Upstate, Lake Placid, NY). Biotinylated donkey antibodies to mouse (1:1000 dilution; Jackson ImmunoReseach Laboratory, Bar Harbor, ME) or goat (1:1000 dilution; Zymed Laboratories, San Francisco, CA) immunoglobulin G were used as secondary antibodies. The biotinylated antibodies were detected with Alexa 488 (Molecular Probes, Eugene, OR) or horseradish peroxidase-conjugated streptavidin. The peroxidase reaction was performed with 3,3-diaminobenzidine (Sigma, St. Louis, MO). Cell nuclei were stained with 2, 4-diamidino-2-phenylindole dihydrochloride *n*-hydrate (DAPI) (0.5 μg ml^{-1}; Sigma) or Mayer's hematoxylin (Wako Pure Chemicals, Osaka, Japan). Samples were observed under an inverted microscope (model IX71; Olympus, Tokyo, Japan). Images were taken by a CCD camera (DP70; Olympus) and post-processed using Adobe Photoshop (Adobe Systems, San Jose, CA).

Immunoblotting

Sample preparation and immunoblot analysis were performed as described [11,13]. Immune complexes were detected by colorimetry with a BCIP/NBT detection kit (Nacalai, Kyoto, Japan).

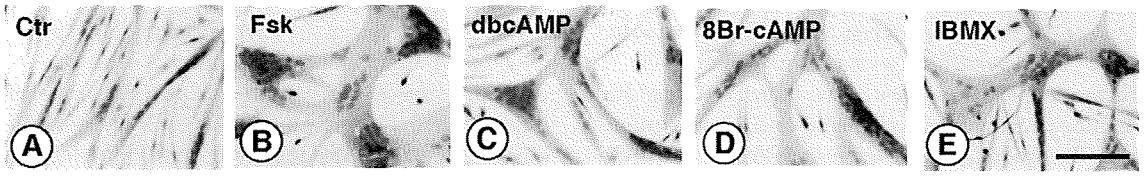

Fig. 1 – Intracellular cAMP-elevating reagents induce muscle cell hypertrophy. (A–E) Ric10 cells (2×10^4 cells per 35-mm dish) were cultured for 36 h in pmDM (A), or in pmDM supplemented with 24 μM forskolin (B), 10 μM dbcAMP (C), 10 μM 8Br-cAMP (D), or 10 μM IBMX (E) to elevate intracellular cAMP levels. Then the cells were subjected to immunostaining for MyHC (brown). Nuclei were counterstained with Mayer's hematoxylin (blue). Images were obtained by bright field microscopy. Scale bar: 100 μm.

Time-lapse recording

Cells were placed in a humid chamber (Olympus, Tokyo, Japan) maintained at 37 °C, and observed under a phase-contrast microscope (IX71, Olympus) with a 10× Plan Apo Fluor objective lens. Time-lapse images were taken with a CCD camera (DP70, Olympus).

Quantification of muscle cell hypertrophy, fusion, and myogenic differentiation

To establish the potentials for cell hypertrophy, fusion, and differentiation, myogenic cells were immunostained with anti-MyHC antibody, and the nucleus was stained with hematoxylin; then at least 1500 nuclei were counted from three randomly chosen areas of three independent cultures. To assess cell hypertrophy, the myotube size was estimated by counting the number of nuclei per cell. The distribution of myogenic cell sizes was determined by calculating the percentage of nuclei in myogenic cells with different numbers of nuclei in the total number of nuclei (myoblasts plus myotubes). The percentage of differentiated cells was measured by calculating the percentage of nuclei in MyHC-positive cells in the total number of nuclei (myoblasts plus myotubes). The incidence of cell fusion, also called the fusion index, was determined by calculating the percentage of nuclei

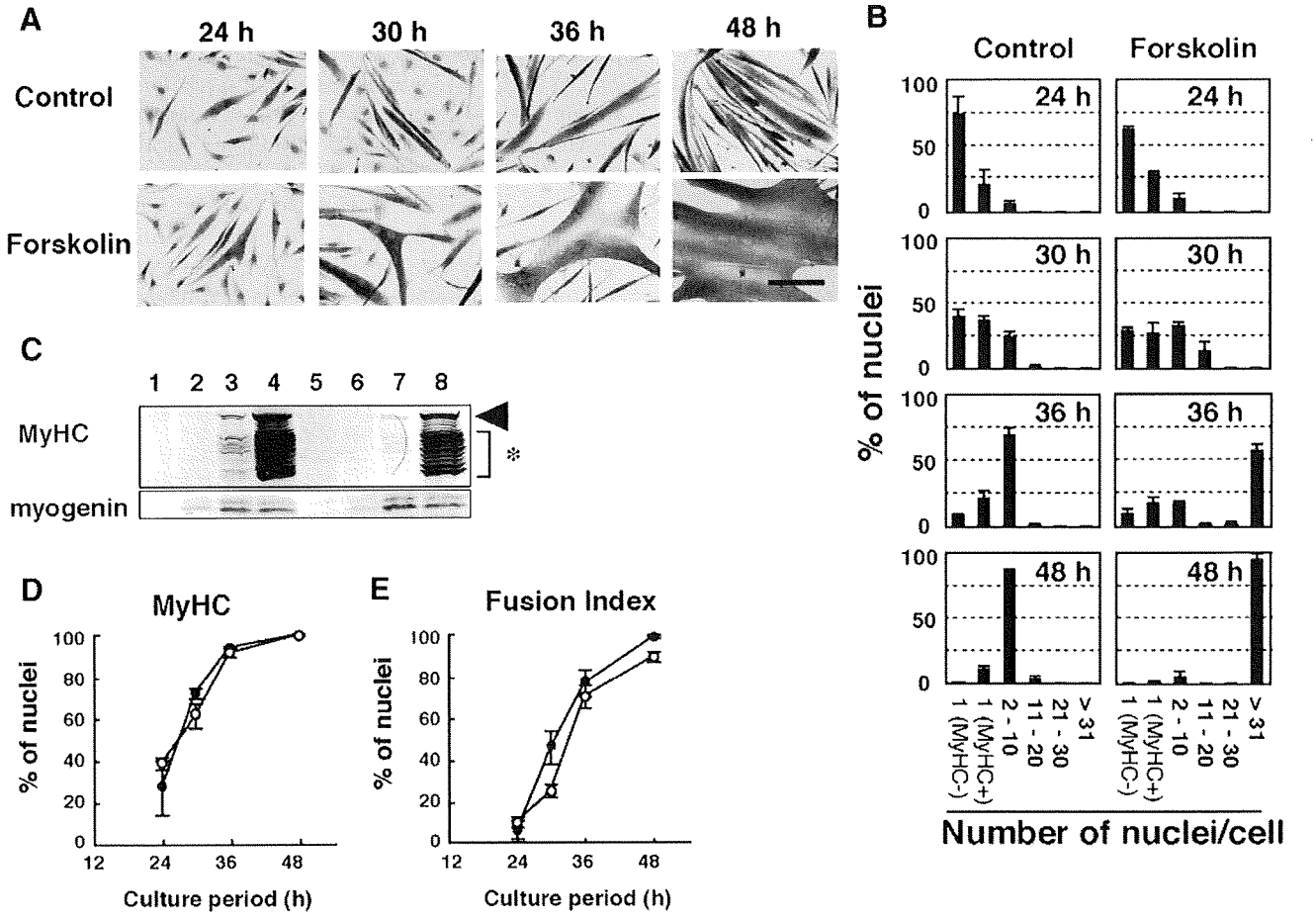

Fig. 2 – Forskolin induces muscle cell hypertrophy but does not enhance cell proliferation and differentiation. Ric10 cells (2×10^4 cells per 35-mm dish) were cultured in pmDM (control) or in pmDM supplemented with 24 μM forskolin for up to 48 h.
(A) The cells were fixed after the indicated periods of culture and subjected to immunostaining for MyHC (brown). Nuclei were counterstained with Mayer's hematoxylin (blue). Images were obtained by bright field microscopy. Scale bar: 100 μm.
(B) Histograms represent the distribution of myogenic cells with different numbers of nuclei in unstimulated (left panels) and forskolin-stimulated cultures (right panels) after the indicated periods of culture. Mononucleated cells were classified to two subpopulations: one expressed MyHC (MyHC+) and the other did not (MyHC–). (C) Total lysates (20 μg of proteins) were prepared from cells that were cultured in the absence (lanes 1–4) or presence of forskolin (lanes 5–8) for 0 h (lanes 1 and 5), 12 h (lanes 2 and 6), 24 h (lanes 3 and 7) or 36 h (lanes 4 and 8), and then subjected to immunoblot analysis for MyHC and myogenin. MyHC is sometimes degraded in 1% SDS-containing lysis buffer by unknown reasons. Arrowhead and asterisk represent full-length and degraded MyHC species, respectively. (D) Differentiated cells were detected by immunostaining with anti-MyHC antibody in unstimulated (open circles) and forskolin-stimulated cultures (filled circles). (E) Fusion indexes were calculated as percentages of nucleus numbers in multinucleated cells of unstimulated (open circles) and forskolin-stimulated (filled circles) cultures. Averages and standard deviations of three independent cultures are shown in panels B, D and E.

in myotubes in the total number of nuclei (myoblasts plus myotubes).

Reagents and peptides

Dibutyryl-cyclic AMP (dbcAMP), 8-bromo-cyclic AMP (8Br-cAMP), and 3-isobutyl-1-methylxanthine (IBMX) were purchased from Sigma. Stearated Ht31 peptide (StHt31S), which is capable of inhibiting PKA anchoring, and its control peptide, StHt31P, were purchased from Promega (Madison, WI). Forskolin (Sigma) was dissolved in ethanol at 24 mM. H89 (Biomol, Devon, UK) was dissolved in dimethylsulfoxide (DMSO) at 10 mM. The other reagents and peptides were dissolved in PBS. Each reagent was diluted with medium immediately before use. For control cultures, the medium was supplemented with the same concentration of vehicle as that used in experimental cultures.

Results

Elevated intracellular cAMP levels induce muscle cell hypertrophy in vitro

We have established a unique primary culture system of mouse myogenic cells derived from muscle satellite cells in adult skeletal muscle [10]. Ric10 is a single cell-derived clone isolated from multiclonal mouse primary cultured myogenic cells, which retains a high capacity for myogenic differentiation. To determine whether cAMP is involved in the regulation of myogenesis, we determined the effects of reagents that elevate intracellular cAMP levels on terminal skeletal muscle differentiation of Ric10 cells in vitro. Ric10 cells were cultured for 36 h in pmDM supplemented with an activator of adenylate cyclase, forskolin, a phosphodiesterase inhibitor, IBMX, or the cAMP analogues 8Br-cAMP and dbcAMP. Ric10 cells gave rise to small bipolar myotubes under differentiation-inducing conditions (Fig. 1A). In contrast, Ric10 treated with the reagents formed large sheet-like multinucleated cells, which we designated "myosheets" (Figs. 1B–E). The results imply that the elevation of intracellular cAMP levels induced muscle cell hypertrophy in vitro.

To elucidate the process of myosheet formation induced by elevated intracellular cAMP levels, Ric10 cells were cultured in pmDM in the presence or absence of forskolin for up to 48 h. No difference in myotube formation was found between unstimulated and forskolin-stimulated Ric10 cells during 24 h of differentiation culture. After 24 h, the size of the myotubes in forskolin-stimulated Ric10 culture increased in proportion to the length of the culture period (Fig. 2A). In control cultures, most myotubes contained 2 to 10 nuclei, and the maximum number of nuclei in myotubes was no more than 20 throughout the culture period (Fig. 2B, left panels). In

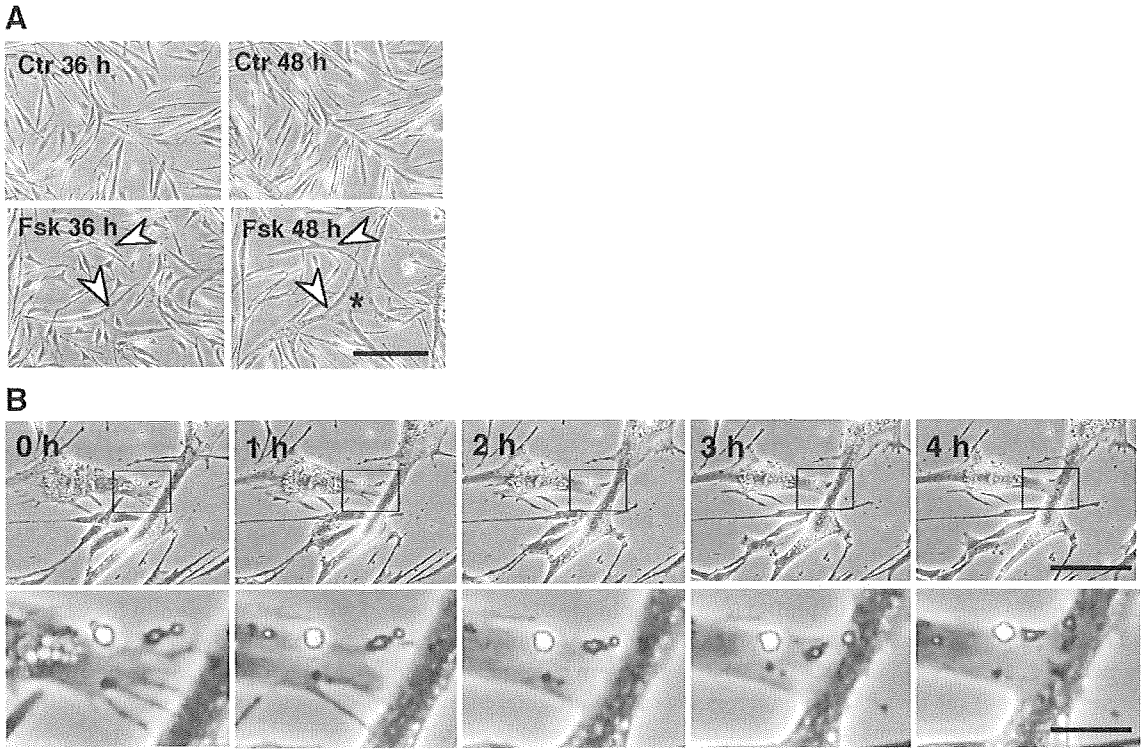

Fig. 3 – Forskolin induces cell fusion between myotubes. Ric10 cells (1×10^4 cells per 35-mm dish) were cultured in pmDM (upper panels in A), or in pmDM supplemented with 24 μM forskolin (lower panels in A and panels in B) for up to 48 h. (A) The same areas of cultures were photographed after 36 and 48 h of differentiation culture. Arrowheads represent myotubes fused with each other to form a large syncytium (asterisk). Scale bar: 100 μm. (B) The process of myotube fusion in Ric10 culture stimulated with forskolin was recorded by phase-contrast, time-lapse microscopy. The lamellipodia of one myotube fused to the lateral plasma membrane of another myotube. Images were obtained at the indicated time points. Squares in the top panels indicate the areas magnified in the bottom panels. Scale bars: 100 μm in top panels; 25 μm in bottom panels.

contrast, forskolin-stimulated Ric10 cells formed extra-large myotubes containing more than 31 nuclei (Fig. 2B, right panels). In forskolin-stimulated culture, more than 90% of nuclei were incorporated into only a few syncytia (Fig. 2A, bottom right panel and Fig. 2B, bottom right panel).

In the next experiments, the effects of forskolin on myogenic differentiation of Ric10 cells were analyzed. Expression patterns of the muscle-specific transcription factor myogenin and the muscle differentiation marker sarcomeric MyHC were similar in unstimulated and forskolin-stimulated Ric10 cells (Fig. 2C). The differentiation index, which represents the ratio of the number of nuclei in MyHC-expressing cells to the total number of nuclei, reached 100% during 48 h of differentiation culture, even in the presence of forskolin (Fig. 2D). In addition, the ratio of the number of nuclei in myotubes to the total number of nuclei, which is called the "fusion index", reached more than 80% after 48 h of culture in the presence or absence of forskolin (Fig. 2E). Therefore, it is unlikely that forskolin affects the myogenic differentiation potential of Ric10 cells. The numbers of nuclei in unstimulated and forskolin-stimulated cultures were 302±64 and 313±11 per mm^2 after 36 h of differentiation culture, respectively, when 2×10^4 cells were plated in a 35-mm dish. The total amounts of cellular protein in unstimulated and forskolin-stimulated cells were 138±32 μg and 125±17 μg after 36 h of differentiation culture when 1×10^5 cells were plated. The results imply that myotube hypertrophy is induced by forskolin independently of stimulation of protein synthesis, cell differentiation, or proliferation. It is noteworthy, however, that fusion of mononucleated progenitor cells was slightly but statistically significantly enhanced in forskolin-stimulated Ric10 cells after 30 h of differentiation culture (Fig. 2E).

Forskolin induces cell fusion between myotubes

Ric10 cells were seeded at low density (1×10^4 cells per 35-mm dish) to slow down the speed of myosheet formation. Then, serial observation of Ric10 differentiation cultures revealed that myosheets were formed through cell fusion between small bipolar myotubes that were stimulated with forskolin (Fig. 3A, lower panels). Although myotube fusion also occurred in control cultures, the incidence was relatively quite low (Fig. 3A, upper panels). The small bipolar myotubes that appeared during the earlier period of differentiation culture formed lamellipodia at their polar ends. Time-lapse recording revealed that myotube-to-myotube fusion in forskolin-stimulated Ric10 cultures always occurred between the leading edge of the lamellipodia of one myotube and the lateral plasma membrane of the other (Fig. 3B and Supplementary data). The results suggest that forskolin enhances cell fusion between myotubes and induces muscle cell hypertrophy, and that lamellipodia of myotubes may retain the capacity for plasma membrane fusion.

Forskolin enhances lamellipodium formation in myotubes prior to cell fusion

A previous study proposed that PKA may be involved in lamellipodium formation of fibroblastic cells [16]. Therefore, the effects of forskolin on the formation of lamellipodia in small bipolar myotubes were determined. Ric10 cells gave rise to small bipolar myotubes containing 2–10 nuclei during 30 h of differentiation culture in pmDM (Fig. 2B). To determine involvement of PKA in forskolin-enhanced lamellipodium formation in myotubes, the small myotubes were cultured for further 6 h with forskolin alone or forskolin plus H89. Forskolin treatment doubled the frequency of lamellipodium formation of unstimulated Ric10 myotubes (Fig. 4A, middle

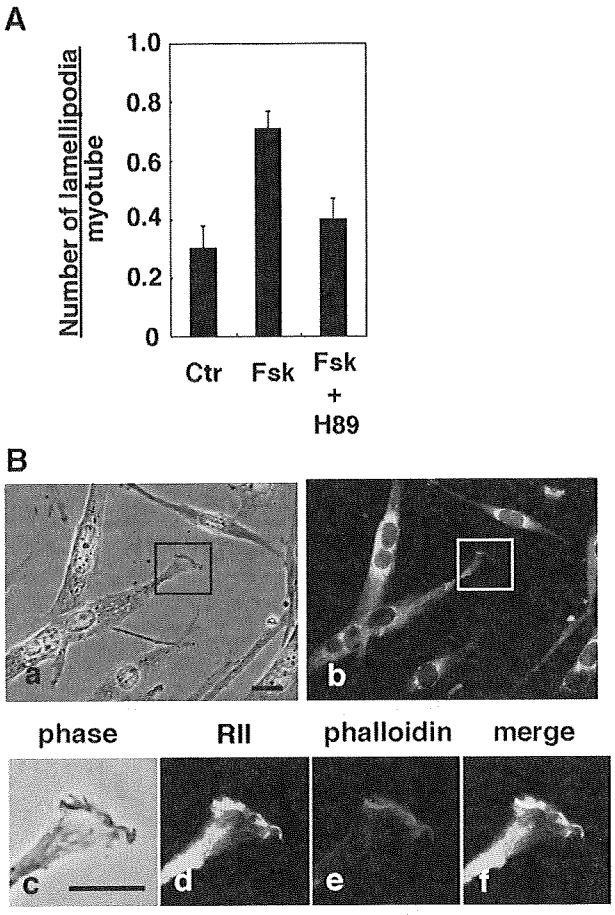

Fig. 4 – Forskolin enhances lamellipodium formation where PKA is located. (A) Ric10 cells (1×10^4 cell per 35-mm dish) were cultured for 36 h in pmDM (Ctr), pmDM supplemented with 24 μM forskolin alone (Fsk), or forskolin plus 10 μM H89 (Fsk+H89). Actin filaments were stained with Alexa Fluor 546-labelled phalloidin. The number of lamellipodia in at least 100 myotubes per dish was counted under a phase-contrast and epifluorescence microscope. Each myotube formed 0, 1, or 2 lamellipodia at their polar ends. Averages and standard deviations of numbers of lamellipodia per myotube from three independent cultures are shown. (B) After 36 h of culture in the medium containing forskolin, Ric10 cells were subjected to immunostaining with anti-PKA RII antibody (RII) (b and d). Actin filaments were stained with Alexa Fluor 546-labelled phalloidin (e). Images in (a) and (c) were obtained by phase-contrast microscopy, and those in (b), (d)–(f) were obtained by epifluorescence microscopy. Cell nuclei stained with DAPI are superimposed in the left panel. (b) Shows the same area in (a). A square in the upper panels represents the area that is magnified in the lower four panels. Scale bars: 20 μm.

column). H89 significantly suppressed the forskolin-enhanced lamellipodium formation (Fig. 4A, right column). Furthermore, immunostaining analysis showed that the type II regulatory subunit of PKA was enriched in the leading edge of lamellipodia where F-actin was accumulated (Fig. 4B), as previously shown in fibroblasts [16]. Taken together with the results here, PKA is likely to be involved in forskolin-enhanced lamellipodium formation.

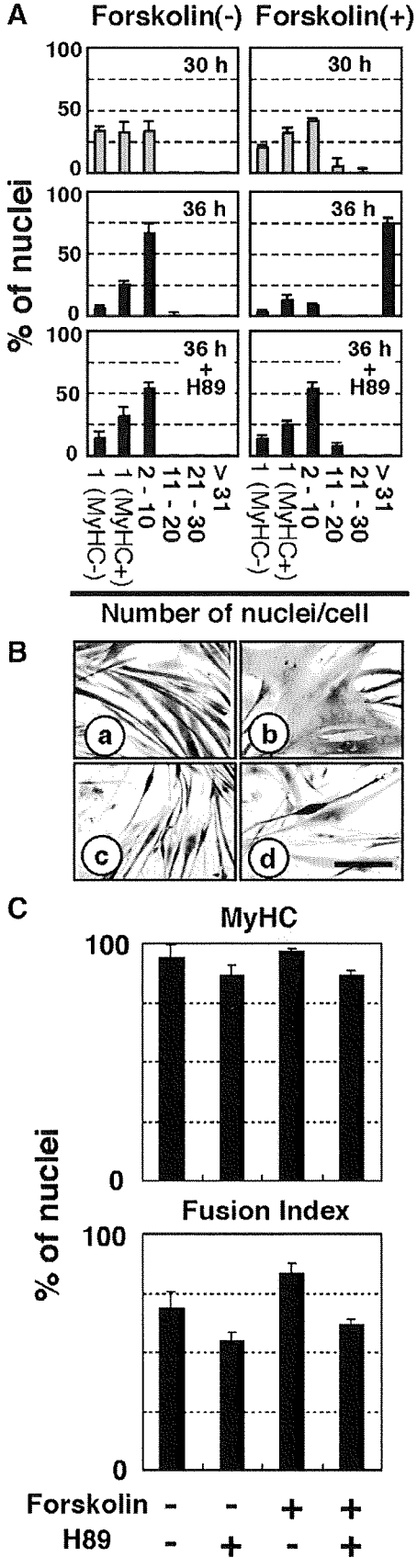

Localized PKA activity is required for forskolin-induced muscle cell hypertrophy

Localization of PKA in lamellipodia of myotubes suggests that blocking PKA activity or anchoring it on these structures will affect forskolin-induced muscle cell hypertrophy. Ric10 cells produced small bipolar myotubes containing 2–10 nuclei during 30 h of differentiation culture in the presence or absence of forskolin (Fig. 5A, upper panels). Then the small myotubes were cultured for further 6 h with forskolin alone or forskolin plus H89 (Fig. 5A, middle and lower right panels, and B). At the end of culture, H89 had prevented myosheet formation in the forskolin-stimulated Ric10 myotube cultures, whereas small and medium-sized myotubes containing 2–20 nuclei had increased in number (Fig. 5A, bottom right panel). The results suggest that the administration of H89 during the last 6 h of culture inhibits mainly forskolin-enhanced cell fusion between small myotubes, resulting in suppression of muscle cell hypertrophy. Both the differentiation and fusion indexes of forskolin-stimulated cultures declined slightly in the presence of H89 (Fig. 5C). However, the reduction of the fusion index or the differentiation index was too small to explain the prevention of myosheet formation in cultures treated with forskolin plus H89 (Fig. 5A, middle and lower right panels). Fusion index was also slightly reduced in the culture treated with H89 alone since H89 inhibited fusion of remnant mononucleated cells during the last 6 h of differentiation culture (Fig. 5C).

In the next series of experiments, stearated Ht31 peptide (StHt31S) was used to inhibit PKA anchoring because it contains a peptide from A kinase anchoring protein (AKAP) and disrupts PKA–AKAP interaction [17]. StHt31S perfectly prevented the muscle cell hypertrophy induced by forskolin,

Fig. 5 – Enzymatic activity of PKA is required for induction of myotube fusion by forskolin. (A and B) Ric10 cells (2×10^4 cells per 35-mm dish) were cultured for 30 h in pmDM (upper left panel in A) or in pmDM supplemented with 24 μM forskolin (upper right panel in A). Then the medium was switched to pmDM supplemented with 0.1% DMSO (middle left panel in A and Ba), forskolin plus DMSO (middle right panel in A and Bb), 10 μM H89 (bottom left panel in A and Bc), or forskolin plus H89 (bottom right panel in A and Bd). After 6 h of further culture, the cells were subjected to immunostaining with anti-MyHC antibody. Nuclei were counterstained with Mayer's hematoxylin. Panels show the distribution of myogenic cells with different numbers of nuclei. Mononucleated cells were classified to two subpopulations: one expressed MyHC (MyHC+) and the other did not (MyHC–). Averages and standard deviations of three independent cultures were shown. Scale bar in panel B: 100 μm. (C) Ric10 cells were treated as described in panel A, and then the potential for differentiation and fusion was analyzed as described in Materials and methods. Averages and standard deviations of three independent cultures are shown.

whereas the control peptide StHt31P, which is incapable of disrupting PKA–AKAP interaction, did not inhibit it (Figs. 6A and B). The forskolin-enhanced lamellipodium formation of small myotubes was suppressed by StHt31S in a similar manner (data not shown).

The decline of the fusion index in StHt31S-treated cells (75.1±7.1% in StHt31P-treated cells versus 51.4±4.8% in StHt31S-treated cells) suggests that StHt31S inhibits cell fusion of mononucleated cells as well as myotubes stimulated with forskolin (Fig. 6C, lower panel). In contrast to the disappearance of myosheets, StHt31S markedly increased the incidence of nuclei in small myotubes in Ric10 cultures treated with forskolin (Fig. 6B). Therefore, the partial inhibition of fusion or differentiation (Fig. 6C, upper panel) of mononucleated cells by StHt31S is unlikely to prevent myosheet formation. We concluded that StHt31S prevents the muscle cell hypertrophy induced by forskolin through suppression of fusion between myotubes. These results suggest that localized PKA activity is required for lamellipodium formation and subsequent cell fusion between myotubes.

In the absence of forskolin, StHt31S also suppressed cell fusion of mononucleated Ric10 cells (64.2±5.6% in StHt31P-treated cultures versus 21.9±5.0% in StHt31S-treated cultures) without significant effects on the expression of MyHC (Fig. 6C) and myogenin (data not shown).

Forskolin induces muscle cell hypertrophy in established and primary cultured myogenic cells

To assess whether myosheet formation enhanced by forskolin is dependent on the type of muscle cells, we determined the effects of forskolin on the myogenic differentiation of a C2C12-derived subclone, COM3 [13], and primary cultured mouse myogenic cells derived from muscle satellite cells [10,14]. COM3 cells differentiated into cylindrical myotubes under the differentiation-inducing condition (Fig. 7A). In contrast, they gave rise to large myotubes when stimulated with forskolin (Fig. 7B). For the assay using primary cultured mouse myogenic cells, colonies derived from single-muscle satellite cells were formed on a 35-mm dish, and then the medium was changed to pmDM. Primary

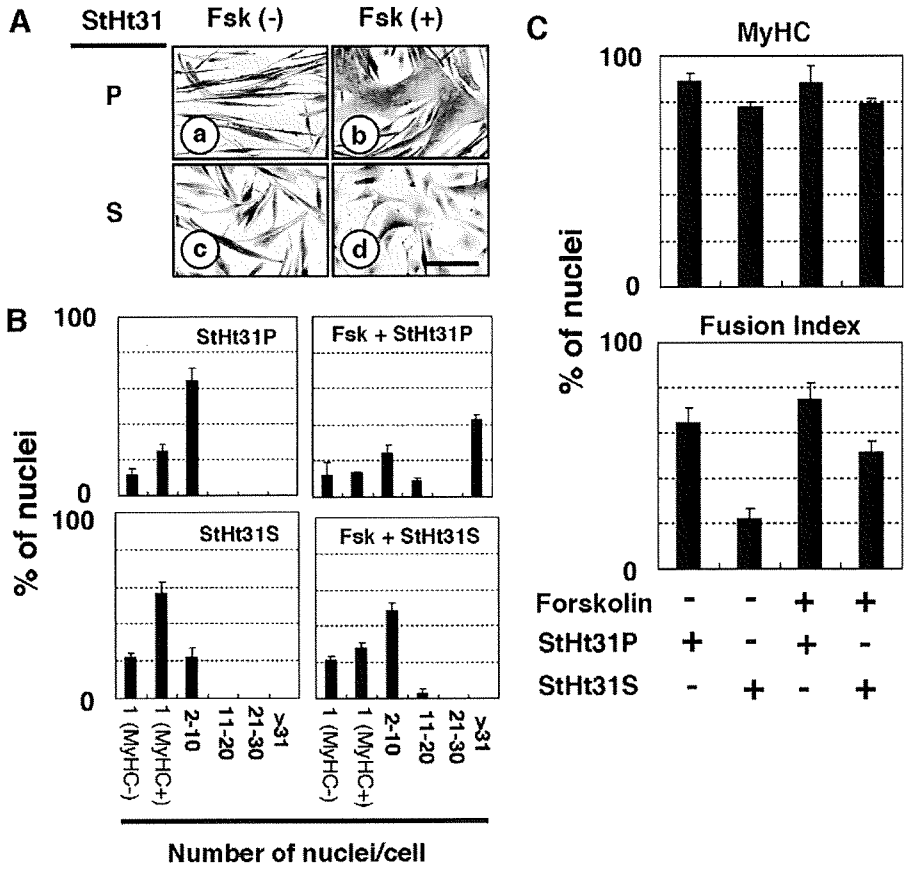

Fig. 6 – Localized PKA activity is required for induction of myotube fusion by forskolin. (A) Ric10 cells (2×10^4 cells per 35-mm dish) were cultured in pmDM (a and c) or pmDM containing 24 μM forskolin (b and d) for 18 h. Then the cells were cultured for further 18 h in medium containing 50 μM StHt31P (a) or StHt31S (c) alone, or forskolin plus 50 μM StHt31P (b) or StHt31S (d). MyHC was immunostained with horseradish peroxidase. Nuclei were counterstained with Mayer's hematoxylin. Images were obtained by bright field microscopy. Scale bar: 100 μm. (B) Panels show the distribution of myogenic cells with different numbers of nuclei in cultures treated as described in panel A. Averages and standard deviations of three independent cultures are shown. (C) Differentiation and fusion potential in cultures treated as described in panel A were analyzed according to Materials and methods. Averages and standard deviations of three independent cultures are shown.